2000

Affects [sic] of ground water velocity on MS2 transport through a sand matrix

Thomas L. Troy
The University of Montana

Affects of Ground Water Velocity on MS2 Transport through a Sand Matrix

by

Thomas L. Troy

B.S., Dickinson College, 1991

Presented in partial fulfillment of the requirements

for the degree of

MASTER OF SCIENCE

in

Geology

The University of Montana

2000

Approved by:

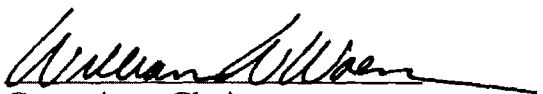

Committee Chair

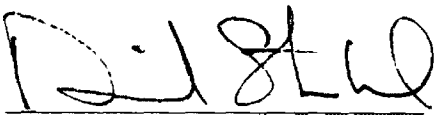

Dean, Graduate School

12-21-00

Date

Troy, Thomas, L., M.S. December 2000 Geology

Affects of Ground Water Velocity on MS2 Transport through a Sand Matrix

Chairman: William W. Woessner

Although numerous studies have investigated how chemical factors affect virus transport, relatively few studies have investigated whether the physical flow system also impacts transport. The influence of flow velocity on one-dimensional MS2 transport in saturated vertical sand columns was investigated. Two continuous flow experiments were conducted using velocities of approximately 12 m/d and 118 m/d. The high flow velocities were designed to approximate the flow velocities encountered in coarse-grained floodplain aquifers and in the vicinity of pumping wells. A mass balance approach was used to assess the relative difference in MS2 attenuation within the columns at each velocity. When the flow velocity was increased by nearly one order of magnitude during continuous virus injection, MS2 concentrations in column effluent increased by nearly two orders of magnitude. It is suspected that virus were exposed to few binding sites at the higher velocity, thus attachment rates decreased. In contrast, virus detachment rates appear to be largely a function of the time that attached virus are exposed to flow as well as the concentration of attached virus. Detachment rates were significantly less than attachment rates for both experiments. Results from this study suggest that virus attachment rates measured from field experiments are not transferable to sites with different flow velocities. Effective virus transport models should contain velocity attachment functions when attempting to predict acceptable setback distances.

Acknowledgments

The National Water Resources Institute, the US EPA, and the University of Montana supported this research. The financial contributions by these institutions to graduate students around the country are paramount to the advancement of science and the development of sound water policy.

I am eternally grateful for the valuable input, support, and patience of my committee chair, Bill Woessner, who I have depended on greatly over the past six years. Bill is a consummate professional who has deeply imprinted upon me the characteristics of an effective educator. Committee members Dan DeBorde and Johnnie Moore provided me with much of the knowledge needed to complete this thesis project through their instruction, review, and constructive suggestions. I also thank Bill Holben who generously agreed to join my committee in the late stages of this thesis project. Pat Ball dedicated countless hours of laboratory instruction for which I am indebted. I also want to thank Nate Stephenson for his assistance in conducting the laboratory experiments. Most importantly, I want to thank my wife, Lisa. Lisa has been an inspiration to me throughout my graduate and professional career and I appreciate her understanding and support.

Table of Contents

List of Tables

List of Figures

Introduction

Infectious viruses have been reported to survive for several months and travel great distances in ground water (Huber et al., 1994; Rossi et al., 1994; Yates et al., 1985; Skilton and Wheeler, 1988). Long-term survival in ground water makes the likelihood of virus capture by downgradient domestic wells high. Consequently, ground water contaminated with sewage waste can lead to considerable health problems including epidemics (Cairncross, 1992; Gerba and Rose, 1990). Common viral pathogens include poliovirus, Norwalk virus, hepatitis A virus, and rotavirus. These viruses are present in the digestive track of infected individuals and they can be released into the ground water by septic systems, leaking sewage lines, and through the process of land farming (where sewage is spread as fertilizer on agricultural fields).

The recently proposed Ground Water Rule (GWR) attempts to ensure the safety of public ground water from microbial pathogens (Macler, 1995). In areas where wastewater treatment systems are not available, the GWR encourages the use of models to predict the flow distance required for pathogen concentrations to fall to acceptable risk limits, this process is referred to as natural disinfection (Macler, 1995). Natural disinfection can occur through pathogen inactivation, physical dispersion, and attenuation within the aquifer. Currently, research is being conducted to characterize pathogen transport behavior under varying environmental conditions. The distance between a source, such as a septic system drain field, and a receiver, such as a well, required for natural disinfection to occur is referred to by regulatory officials as the setback distance.

In order to determine safe setback distances for various hydrogeologic and chemical environments, researchers are formulating predictive models based on coliphage (viruses that infect and replicate in coliform bacteria) transport behavior (Bales et al., 1997; Yates et al., 1987; Rossi et al., 1994). The use of coliphage as models for enteric viruses is necessary, as the release of enteric viruses into ground water systems for controlled field experiments is usually not permitted. Also, the detection of pathogenic viruses at possible regulatory levels is currently not feasible (Macler, 1995). Coliphages MS2, PRD-1, and ΦX-174, among others, have been used most commonly by researchers in ground water transport studies as surrogates for water-borne viral pathogens (DeBorde et al., 1998; Bales et al., 1991, 1993, and 1995). These coliphage are similar in size (20 - 62 nm), surface characteristics (isoelectric points of 3 - 6), and survival rates to viral pathogens (Bales et al., 1995).

The principal mechanisms that cause virus concentrations in ground water to decrease naturally in the direction of flow include inactivation, attachment to aquifer material and the physical spreading (advection-dispersion) processes (Bales et al., 1989; Zerda et al., 1985; Chyrsikopoulos and Sim, 1996). Temperature is the predominant factor that influences virus inactivation, as noted by Yahya et al. (1993). They found that virus inactivation occurred rapidly (i.e. days) at 23 °C and slowly (i.e. months) at 7 °C. Unlike virus inactivation, the process of virus attachment is considerably more complex.

Viruses attach, or sorb, to the solid matrix under favorable environmental conditions and they can be dislodged, or detached if the favorable conditions are altered. The extent to which the attachment process is reversible and irreversible depends on the

aqueous chemistry, the properties of the virus and aquifer material, and the physical flow system. Researchers have attempted to identify and quantify many factors that may potentially affect the attachment of virus within the subsurface.

Experiments conducted by Bales et al. (1991) demonstrated accelerated MS2 detachment when pH values and concentrations of beef extract were increased. Alhajjar et al. (1988) observed rapid virus attachment in environments with high ionic strength waters and slow detachment in waters with a decreased ionic strength. Pieper et al. (1997) found that the presence of sewage-derived organic matter also plays an important role in virus transport, attachment decreasing with an increasing organic content.

The effect of the physical flow system on virus and bacteria attachment has also been investigated. Several laboratory studies have demonstrated that the rate of microorganism attachment to granular aquifer material is inversely related to flow velocity. Smith et al. (1985) observed that less *Escherichia coli* was retained in silt-rich unsaturated soil at flow velocities of 0.96 meters/day (m/d) than at 0.12 m/d. Wollum and Cassel (1978) studied the transport of *Streptomycete condia* in saturated sand columns at flow velocities of 3.5 m/d and 8.9 m/d. They found that less streptomycete was retained within their column at the higher flow velocity. Tan et al. (1994) observed a similar relationship between velocity and *Pseudomonas sp.* transport for velocities of 4.3 m/d and 17.3 m/d in saturated sand columns.

Some researchers have speculated that velocity may only have an effect on the transport of microorganisms over a variable and finite range, which depends on the physical and chemical system. Wang et al. (1981) conducted experiments in saturated,

predominantly sand columns. They found that increasing the flow velocity from 0.33 to 3.14 m/d significantly decreased the rate of poliovirus type 1 and echovirus type 1 attenuation; no significant difference in attenuation occurred when the flow velocity was increased from 3.14 to 13.52 m/d. Lance and Gerba (1980) similarly observed that less poliovirus type 1 was attenuated within coarse sand columns at flow velocities of 1.2 m/d than 0.6 m/d; there was not a significant difference in the poliovirus retained within the column when the velocities were increased from 1.2 m/d to 12 m/d. Yan et al. (1997) found flow velocities of 0.206 and 0.842 m/d did not effect MS2 attachment in saturated sand columns.

No studies have investigated microorganism transport through granular soils at the upper limits of ground water flow velocities, such as those found in gravel- and cobble-dominated floodplain aquifers and in the immediate vicinity of a pumping well. The only study that was performed at high flow velocities occurred in fractured material (Harton et al., 1998). MS2 and PRD1 transport was evaluated in a highly weathered and fractured shale saprolite. They found that less PRD-1 and MS2 were retained at a maximum fracture flow velocity of 210 m/d than at a minimum fracture flow velocity of 0.49 m/d.

Another process that has rarely been investigated is the effect of flow velocity on microorganism detachment. Harton et al. (1998) observed brief spikes in PRD-1 and MS2 concentrations when the maximum fracture flow velocity was increased from 0.49 m/d to 210 m/d using a virus-free injectate. They concluded that bacteriophage attachment was largely irreversible under the conditions of their study.

The research reported here was designed to establish the relationship between ground water velocity and the rates of virus attachment and detachment under high flow velocity conditions. To investigate the effect of flow velocity on virus transport, all of the factors that could potentially influence virus transport were controlled, except for flow velocity. This was accomplished through two continuous injection experiments, each was conducted in a vertical up-flow sand column set up in a controlled temperature room (4°C +/-1 °C). Two different flow rates were applied to the columns to test the affect of flow rate on virus transport. The goal of one experiment (Experiment 1) was to determine the affect of flow rate on virus attachment and detachment. The goal of another experiment (Experiment 2) was to determine the affect of flow rate on virus detachment.

Flow velocities of approximately 12 to 118 m/d were used in each experiment. These velocities were designed to be similar to ground water flow velocities found at the Erskine field site in Western Montana (Woessner et al., 1998) (Figure 1). Woessner et al. (1998) found that virus plumes traveled at rates up to 30 m/d along preferential flowpaths in the high hydraulic conductivity material. The question addressed by my research was: Does flow velocity influence virus transport in a sand matrix?

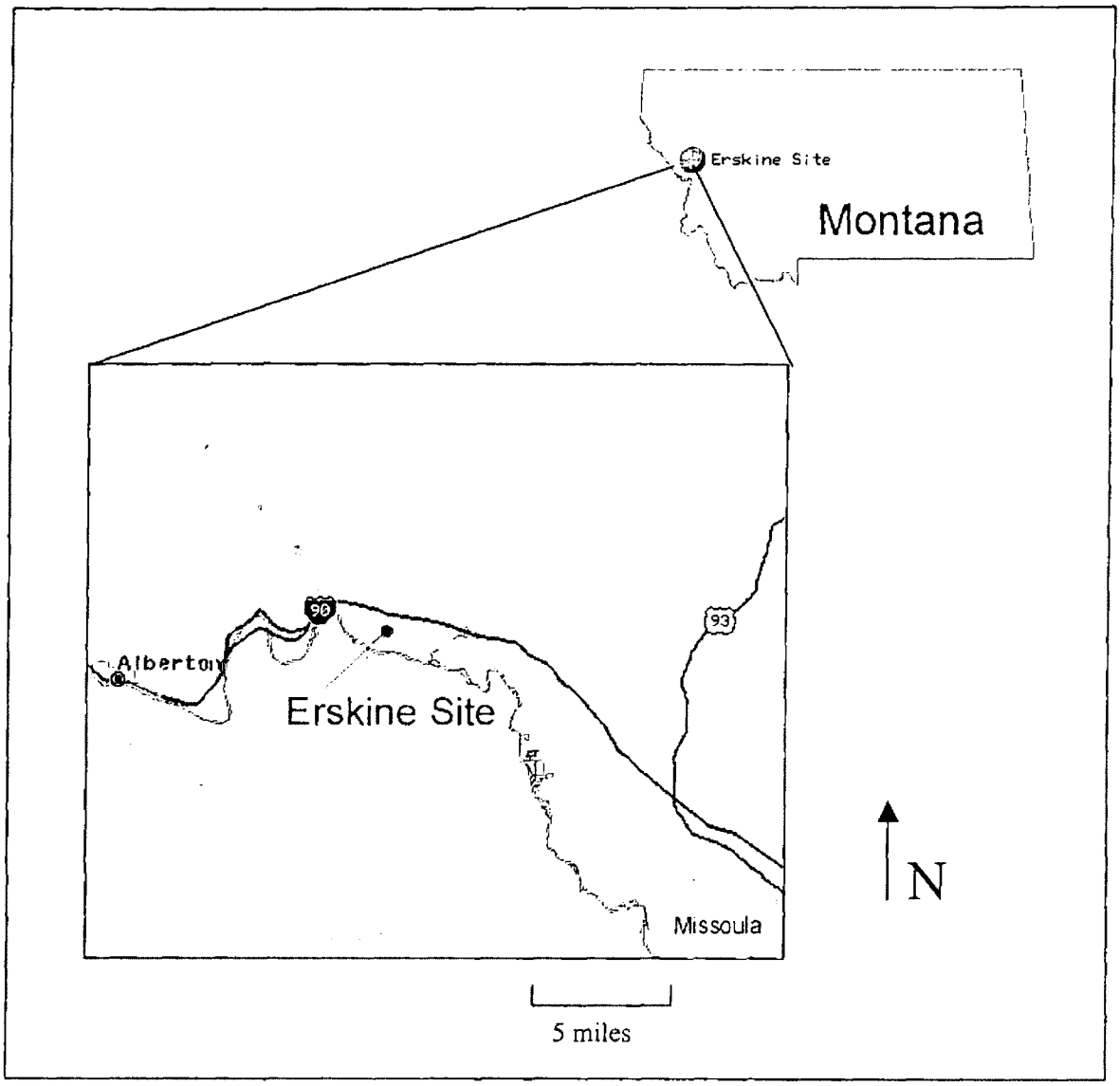

Figure 1. Erskine site location map.

Bacteriophage MS2 was used in this study. MS2 is a member of what is called "male specific" bacteriophage. Sampling this group of viruses in ground water has been proposed under the Ground Water Rule. The presence of "male specific" viruses are believed to be a good indicator for pathogenic microorganisms. MS2 is an icosahedral bacteriophage with a diameter of approximately 24 nm (Dowd et al., 1998) and its' isoelectric point occurs at a pH of 3.5 (pH_{iep}) (Penrod et al., 1996). Solution pH values above 3.5 result in MS2 having a net negative surface charge.

Based on the findings of previous studies, and my preconceptions, I anticipated four likely relationships between flow velocity and MS2 attachment and detachment. Regarding virus attachment, I anticipated that as flow velocity increased, there would either be less MS2 attachment or there would be no effect on MS2 attachment. Regarding virus detachment, I anticipated that as flow velocity increased, there would be either increased MS2 detachment, or there would be no effect on MS2 detachment.

Materials and Methods

Column Materials and Construction

Two continuous injection sand column tracer experiments were conducted in dedicated vertical up-flow columns (Figure 2). Tygon tubing, serving as influent and effluent lines, was connected to the base and top of the columns with brass fittings. Two flexible vinyl standpipe piezometers were affixed to the lower and upper portion of each column. All connections to the column were fitted with fine nylon mesh to contain the sand. Both columns were constructed of PVC pipe and had dimensions of 1.23 m in length and 7.62 cm inner diameter. A variable speed peristaltic pump was used to control the flow into the columns.

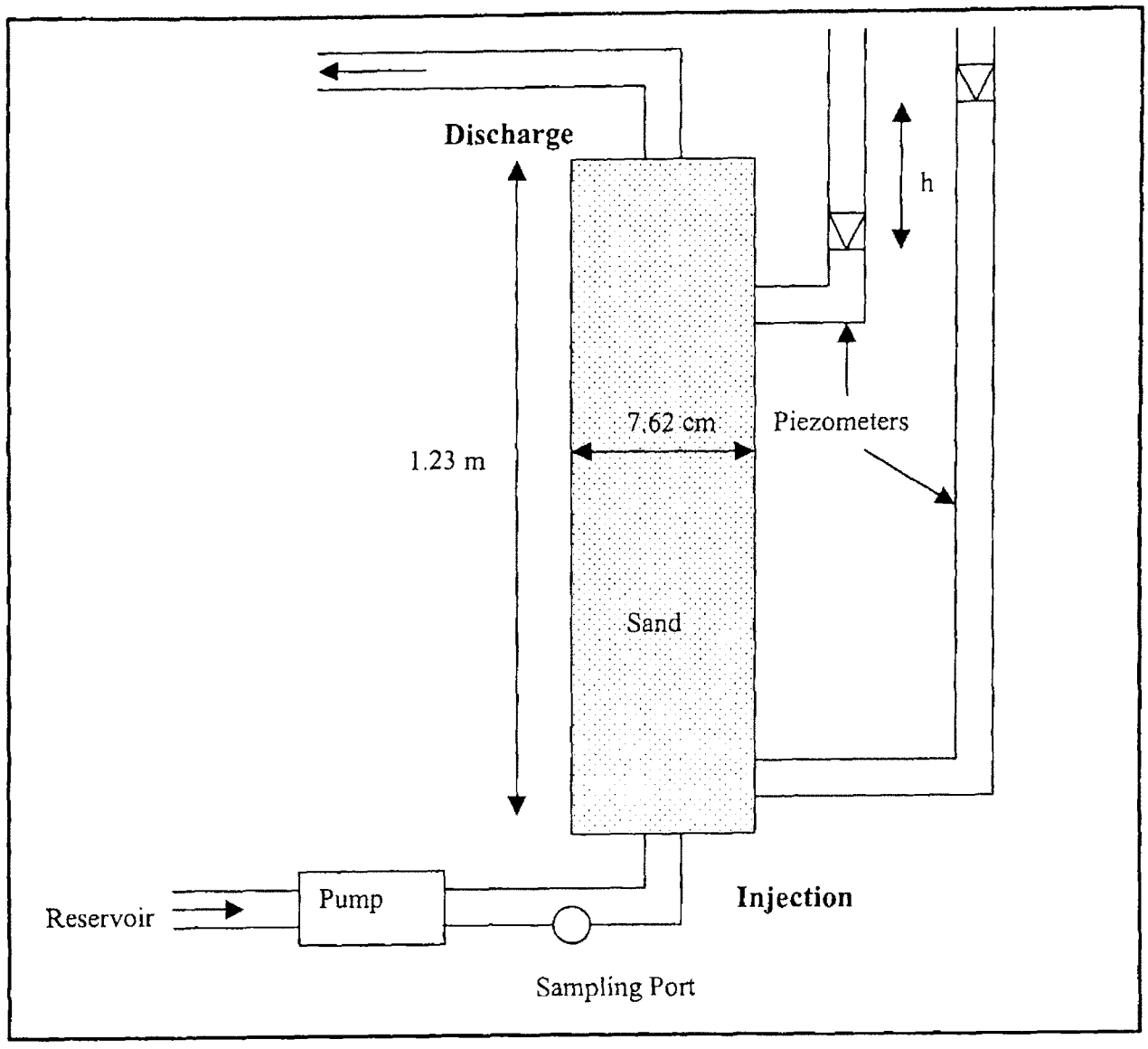

Figure 2. Column experimental setup.

The sand used for both experiments was obtained from a local gravel yard. The material was air dried and sieved to a medium to coarse-grained sand. The mean grain size of the sand was 0.46 mm with a uniformity coefficient of 1.5. The well-sorted sand was composed predominantly of quartz and it did not have any visible signs of metal-oxide coatings or organic carbon. The sand was gravity-packed into the columns using the tap and fill method. The hydrogeologic properties of the columns are presented in Table 1. Based on the hydraulic gradient calculated from the piezometers, the discharge rate, and the dimensions of the column, the hydraulic conductivities for Experiments 1 and 2 were 43 m/d and 52 m/d, respectively. Considering hydraulic conductivity values can vary over several orders of magnitude, these values are in good agreement with the hydraulic conductivity values calculated from the mean flow velocities derived from bromide breakthrough curves, which were 36 and 39 m/d for Experiments 1 and 2, respectively. The hydraulic conductivity values calculated from the column piezometers and bromide breakthrough curves were averaged. This average hydraulic conductivity value was used in this study.

Table 1. Column hydrogeologic properties and site water chemistry.

Hydrogeologic Properties	Experiment 1	Experiment 2
Porosity	0.37	0.37
Gradient (@ low velocity)	0.14	0.12
Average K (m/d)	40	46
Low GW velocity (m/d)	14	12
High GW velocity (m/d)	118	105
Pore Volume (L)	2.1	2.1

Water Chemistry	
Conductivity (μS/cm)	288
Dissolved Oxygen (mg/l)	3.5
pH	7.2
Temperature (°C)	5.0
Ca (mg/l)	53.7
Mg (mg/l)	16.7
Na (mg/l)	8.6
K (mg/l)	2.3
Fe (mg/l)	0.01
Br (mg/l)	<0.1
Cl (mg/l)	7.3
SO_4 (mg/l)	16.3
HCO_3 (mg/l)	249
NO_3-N (mg/l)	0.66
Dissolved Organic Carbon (mg/l)	2.1

Column Preparation

The columns were refrigerated in a controlled temperature room at 3-5 °C and they were conditioned for approximately 5 pore volumes (PV) (a pore volume refers to the volume of water required to saturate the column) with ground water (site water) obtained from a background well at the Erskine experimental field site in western Montana (Woessner et al., 1998). The site water chemistry is provided in Table 1. The water was collected and stored at 3-5 °C. The columns were saturated from the bottom at a pumping rate of 19 ml/min to allow air to escape through the tops of the columns. After 2 PV of site water were injected into the columns at 19 ml/min, the pumping rate

was increased to 200 ml/min for 2 PV, and then the flow rate was decreased to 19 ml/min for an additional pore volume. The columns were subjected to both pumping rates to physically condition the sand pack prior to adding the injectates.

Column Experimental Procedures

Both experiments were conducted using site water at temperatures of 3-5 °C (to minimize MS2 deactivation), and flow velocities of approximately 12 and 118 m/d. Experiments 1 and 2 contained 5 and 7 stages, respectively. Each stage delineates a change in either the flow rate or injectate composition. Stages 1, 3, 4, and 6 were conducted at a pumping rate of 19 ml/min, which is equivalent to a mean flow velocity of approximately 12 m/d. Stages 2, 5, and 7 were conducted at a pumping rate of 200 ml/min, which is equivalent to a mean flow velocity of approximately 118 m/d (Table 2). The pumping rates were frequently checked volumetrically and monitored using standpipe piezometers. They were adjusted as needed and maintained within +/- 10% of the targeted rates. Table 2 describes the pumping schedule for each experiment. Periodic measurements of influent and effluent temperature and pH were collected over the duration of the experiments using an Orion pH electrode and meter. Both temperature and pH remained at 4°C +/- 1°C and 7.2 +/- 0.1, respectively, throughout the experiments.

Table 2. Injectate composition and injection schedule.

	Stage 1	Stage 2	Stage 3	Stage 4	Stage 5	Stage 6	Stage 7
Experiment 1							
Flow Rate (ml/min)	19	200	19	19	200	NA	NA
Flow Velocity (m/d)	14	118	14	14	118	NA	NA
Bromide Conc. (mg/l)	19.6	36.6	36.6	0	0	NA	NA
MS2 Conc. (PFU/ml)	70.5	70.5	70.5	0	0	NA	NA
Pore Volumes	13.6	14.9	14.9	21.7	10.4	NA	NA
Experiment 2							
Flow Rate (ml/min)	19	200	19	19	200	19	200
Flow Velocity (m/d)	12	105	12	12	105	12	105
Bromide Conc. (mg/l)	13.1	13.1	13.1	0	0	0	30.0
MS2 Conc. (PFU/ml)	26,800	26,800	26,800	0	0	0	0
Pore Volumes	14.7	15.2	14.9	11.9	11.4	9.3	2.8

Experiment 1 Injectate

The injectate used for Stages 1-3 of Experiment 1 was composed of site water spiked with 70.5 PFU/ml (plaque forming units/ml) of MS2 (Table 2). Stage 1 also contained 19 mg/l bromide and Stages 2 and 3 contained 36 mg/l bromide. Immediately following the completion of Stage 3, only site water was continuously injected. Generally 10 to 15 PV of injectate was passed through the column during each stage (Table 2). Bromide data were used to calculate mean flow velocities, to provide an independent means of calculating hydraulic conductivity, to determine the time required for the flow systems to physically equilibrate, and to compare bromide and MS2 breakthrough curves.

Experiment 2 Injectate

The injectate used for Stages 1-3 of Experiment 2 was composed of site water spiked with 2.68×10^4 PFU/ml MS2 and 13.1 mg/l bromide. Immediately following the completion of Stage 3 only site water was continuously injected, with the exception of Stage 7 where a spike of 30.0 mg/l bromide was added. The injectate composition and

injection schedule for Experiment 2 is provided in Table 2. Generally 10 to 15 PV of injectate was passed through the column during each stage (Table 2).

Sample Collection and Analysis

Bromide samples were collected in sterile 50 ml polypropylene bottles and MS2 samples were generally collected in sterile 15 ml centrifuge vials. When low MS2 concentrations were anticipated, 50 ml centrifuge vials were used. Effluent bromide and MS2 samples were collected from the Tygon tubing affixed to the tops of the columns. Bromide and MS2 injection concentration (C_o) samples were collected in-line between the pump and the base of the columns. All MS2 samples were immediately placed on ice after collection and stored at 4°C until analysis within six days. Four replicate samples of the injection concentration were collected during each experiment. MS2 inactivation was not observed during either Experiment 1 or 2 and it is considered to be negligible due to the low temperatures and short duration (less than 72 hours) of both experiments and the limited holding time (Yates et al. 1985 and 1987). The weighted mean C_o was used for all calculations for both experiments.

Bromide was analyzed within one week of collection using a bromide-specific electrode. Ten percent of the bromide samples were duplicates and the replicate sample error was less than 5%.

MS2 samples were assayed using the method described by DeBorde et al. (1998). This method was slightly modified to accommodate the low MS2 concentrations observed during Stages 4 and 5 of Experiment 1. Instead of plaquing 10 ml of sample for

Stages 4 and 5, 40 ml of sample were plaqued. Only dilutions that resulted in 10 – 300 plaques per plate were counted. Almost all replicate samples collected during Experiments 1 and 2 were quadruplicates. Twenty-five percent of the samples collected during Experiment 1 were replicates and 17% of the samples collected during Experiment 2 were replicates. Replicate sample error was calculated as %RSD (Relative Standard Deviation). The error for each experiment was calculated as the mean %RSD of all replicate samples collected during each experiment. The mean error for Experiment 1 was 28% and for Experiment 2 it was 19%. The relatively high error for Experiment 1 can be attributed to the low PFU counts per sample during Stages 1, 4, and 5.

Calculation of Collision Efficiency

The relative breakthrough (RB, %) of MS2 was calculated using the procedure described by Harvey and Garabedian (1991). Relative breakthrough is a measure of the degree of virus attenuation by attachment to aquifer material. It is the ratio of the time-integrated mass of virus to that of a conservative tracer. The attenuation (%) of MS2 is 100 – RB.

The number of collisions between MS2 and sand grains that result in attachment was also estimated by calculating the collision efficiency factor (α), which is based on colloid filtration theory of kinetically controlled irreversible attachment (Harvey and Garabedian, 1991).

$$\alpha = d\{[1-2(\alpha_L/x)\ln(RB)]^2 - 1\} / 6(1-\theta)\eta\alpha_L$$

where d is the average grain diameter (L), α_L is the longitudinal dispersivity (L), x is the transport distance (L), θ is the porosity, and η is the single collector efficiency caused by Brownian motion (dimensionless). Pieper et al. (1997) defined η as:

$$\eta = 0.9A_s^{1/3}[(k_bT/\mu d_p dv)]^{2/3}$$

where A_s is the Happel sphere-in-cell model correction factor, k_b is the Boltzmann constant (1.38×10^{-23} J mol^{-1} K^{-1}), T is absolute temperature (K), μ is the dynamic viscosity [mass/(Lt)], d_p is the virus diameter (L), d is the average grain diameter (L), and v is the fluid velocity (L/t). A_s is calculated where $\varepsilon = (1 - \theta)^{1/3}$:

$$A_s = 1 - \varepsilon^5/(1 - 1.5\varepsilon + 1.5\varepsilon^5 - \varepsilon^6).$$

Results

Experiment 1

MS2 and bromide concentrations for Experiment 1 were plotted against the elapsed number of pore volumes in Figure 3. The MS2 data points presented in Figures 3 and 5 are somewhat variable due to small chemical and/or physical perturbations in the system as well as analysis error. Other researchers (Harton et al., 1998, Bales and Li, 1997, and Hinsby et al., 1996) have commonly observed this variability in MS2 concentration.

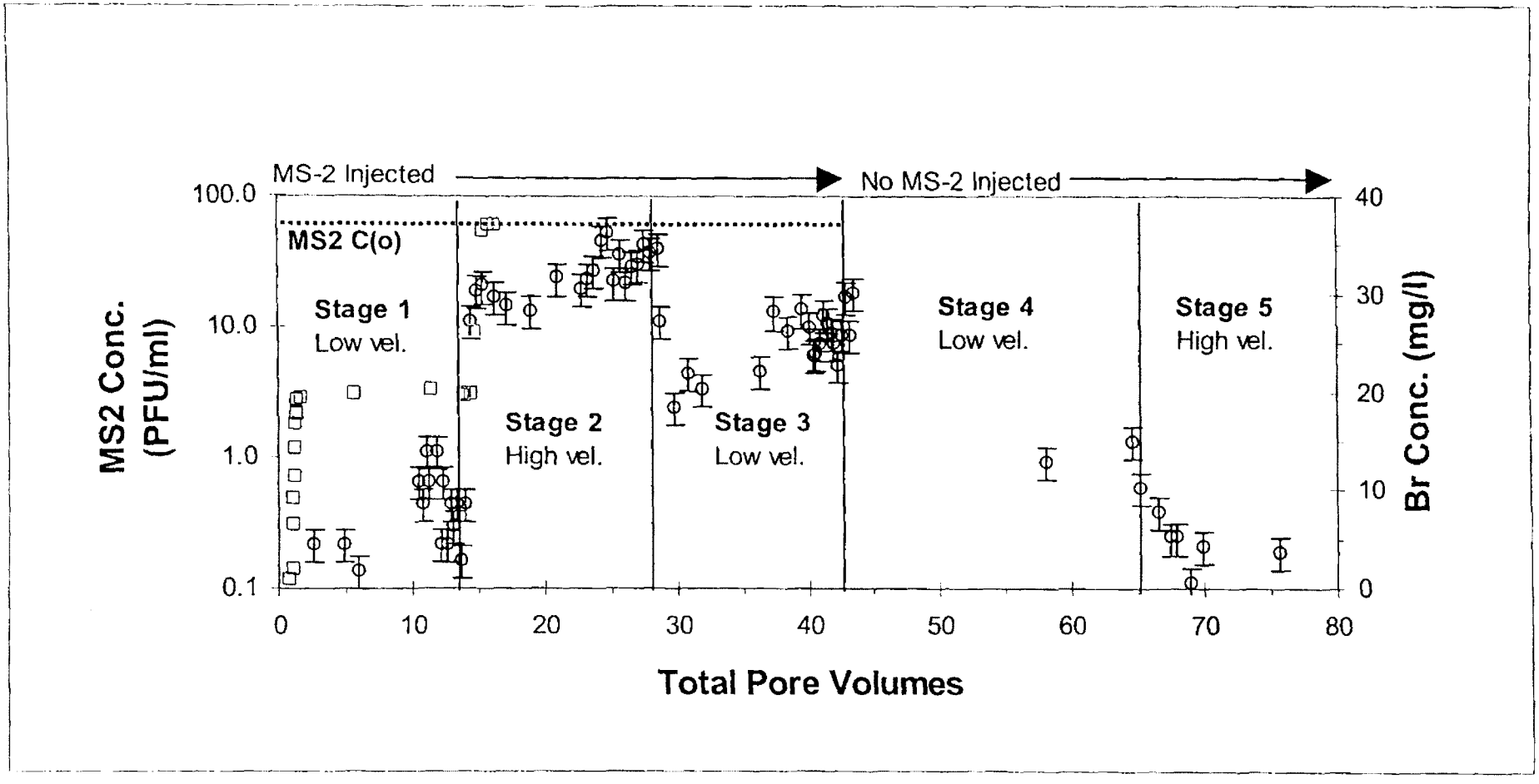

Figure 3. Bromide (□) and MS2 (o) concentrations over total pore volumes for Stages 1-5 of Experiment 1.

Bromide spikes were first detected in Stages 1 and 2 at approximately 0.7 and 1.1 PV, respectively, and they peaked after 1.4 PV in Stage 1 and 1.7 PV in Stage 2. The average flow velocity within the column at each pumping rate was calculated using the time required for 50% of the injected bromide concentration to be reached. Average flow velocities for Experiment 1 are provided in Table 2.

During MS2 injection (Stages 1-3), virus concentrations were highest during the high flow rate (Stage 2) and lowest during the low flow rate (Stages 1 and 3). MS2 concentrations generally fluctuated from 0.2 to 1.0 PFU/ml for Stage 1 and then at the beginning of Stage 2, MS2 concentrations increased rapidly by nearly two orders of magnitude to fluctuate between 20 and 50 PFU/ml. Concentrations remained fairly consistent until Stage 3 when, at the low flow rate, concentrations decreased to fluctuate from 3.0 to 20 PFU/ml.

Nearly 15 PV of virus-free solution were flushed through the system at the low flow velocity (Stage 4) to allow the aqueous phase MS2 still in transit through the column to be evacuated. The virus recovered from the column after 58 total pore volumes are presumed to have undergone the attachment and detachment processes. After the injectate was changed to only site water at the beginning of Stage 4, MS2 concentrations decreased to approximately 0.6 PFU/ml after 22 PV had elapsed. At the initiation of Stage 5, the flow rate increase resulted in rapidly decreasing MS2 concentrations for the first 4 PV and then the concentrations stabilized at 0.2 PFU/ml. Since the MS2 concentrations during Stages 4-5 are near the analytical detection limit for

the volume of sample collected, conclusions drawn from the data must be considered inconclusive.

Mass Balance

A mass balance approach was used to illustrate trends in the partitioning of mass at different flow rates. The mass retained within the column (cumulative mass injected less cumulative mass recovered) was plotted against PV in Figure 4. Bromide breakthrough curves demonstrate that the flow system reached a physical equilibrium after approximately 2 pore volumes. To ensure steady state conditions were met at each flow rate, linear regression lines were applied to data points after 2 to 4 PV had elapsed for each stage. The slopes of linear regression lines were used to determine attachment rates. Since the processes of attachment and detachment occurred concurrently throughout the experiment, MS2 attachment and detachment rates could not be isolated from the overall process. For this reason, MS2 transport is characterized by the net attachment rate. Net attachment rates discussed in this study are the net result of all interactions between the MS2 column population and the total number of available binding sites within the column.

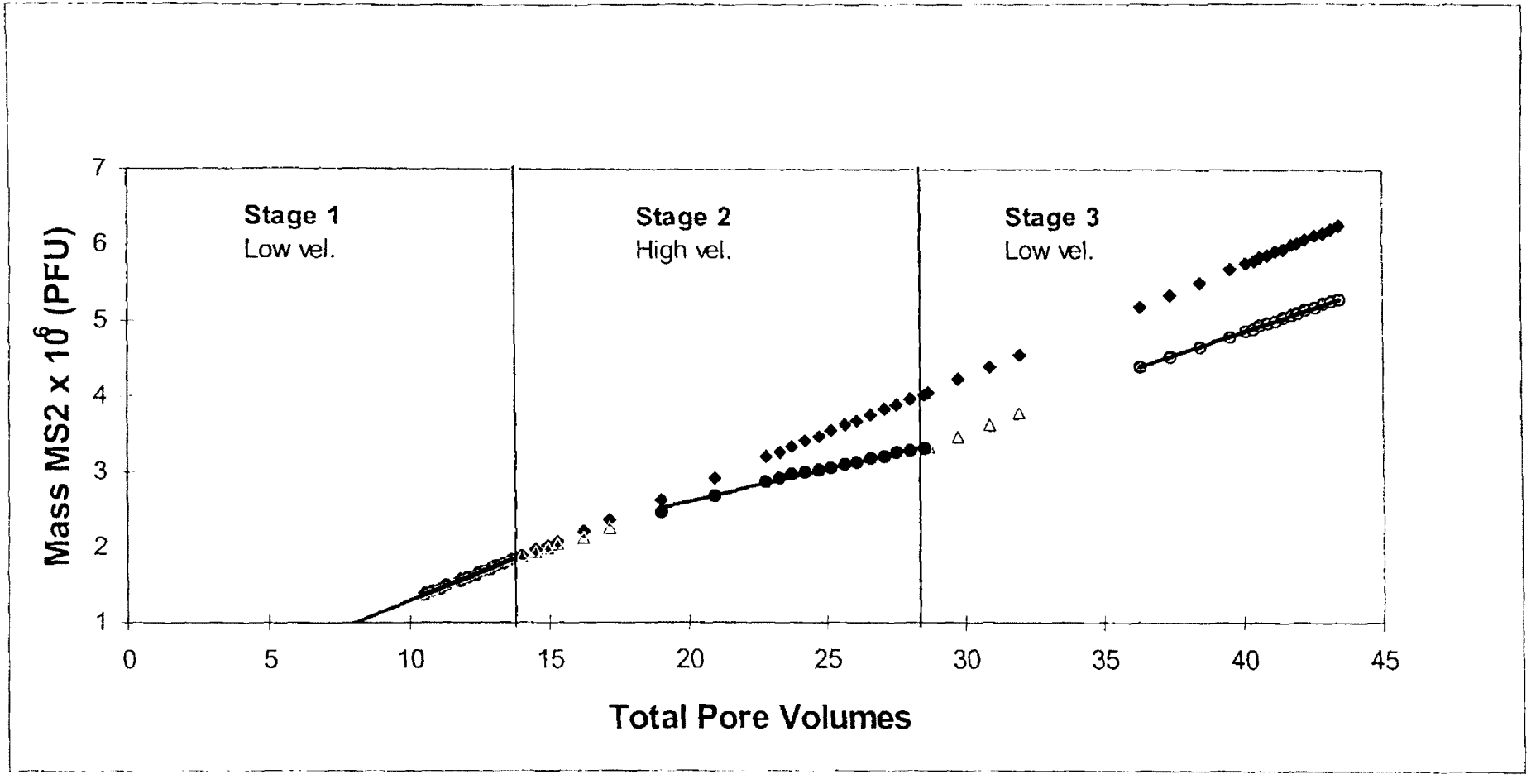

Figure 4. Cumulative mass of MS2 injected (◆) and cumulative mass of MS2 retained (●) over total pore volumes for Stages 1-3 of Experiment 1. Regression lines were not calculated using data points (Δ) collected within four pore volumes after a flow rate change.

The MS2 data from Experiment 1 was analyzed with respect to the cumulative mass of MS2 injected into, and retained within, the column. Figure 4 shows the results of a mass balance analysis on Stages 1-3 and the slopes of the regression lines are summarized in Table 3. MS2 was injected at a rate of 1.48×10^5 PFU/PV over Stages 1-3. During Stage 1 the net attachment rate of MS2 was 1.47×10^5 PFU/PV, which is very similar to the rate at which MS2 was injected. During the high flow velocity of Stage 2, the rate at which MS2 was retained within the column substantially deviated from the injection rate. When the flow velocity was increased to 118 m/d the rate at which MS2 was retained within the column decreased to 8.68×10^4 PFU/PV. This can be attributed to either a decreased rate of attachment, increased rate of detachment, or a combination of these rates. The net attachment rate for Stage 3 was more similar to the injection rate than Stage 2. When the flow velocity was decreased to 14 m/d the rate at which MS2 was retained within the column increased to 1.27×10^5 PFU/PV. This may be due to an increased rate of attachment, a decreased rate of detachment, or a combination of these two.

Table 3. Summary of Experiment 1 linear regression line slopes. (PFU/PV)

Stages	Experiment 1
Inj. Rate	1.48×10^5
1	1.47×10^5
2	8.68×10^4
3	1.27×10^5

Tables 4 and 5 summarize the MS2 mass distribution over discrete time intervals for the continuous MS2 injection and MS2-free injection portions of the experiment, respectively. In Table 4, the number of MS2 injected into the column was estimated by

multiplying the MS2 C_o by the volume of injectate exposed to the column over a given two-hour period under steady state conditions. The number of MS2 attached to the porous media was estimated by subtracting the mass of MS2 recovered (based on the effluent MS2 concentration) from the mass injected over the respective two-hour period. The number of attached MS2 in the two-hour period is also expressed as a percentage in Table 4.

Table 4. MS2 mass distribution over two-hour period.

Stage	MS2 Attached (PFU/2 hr)	MS2 Injected (PFU/2 hr)	Attached/Injected
1	1.5×10^5	1.5×10^5	100 %
2	1.1×10^6	1.7×10^6	65 %
3	1.4×10^5	1.6×10^5	88 %

In Table 5, the number of MS2 detached from the column over a given one-hour period during steady state conditions was estimated by subtracting the number of MS2 purged from the column (based on the effluent MS2 concentration) from the estimated number of MS2 attached within the column at the beginning of the one-hour interval. The number of detached MS2 is also expressed as a percentage in Table 5.

Table 5. MS2 mass distribution over one-hour period for Experiments 1 and 2.

	Experiment 1		Experiment 2	
Stage	MS2 Detached (PFU/hr)	% MS2 Detached	MS2 Detached (PFU/hr)	% MS2 Detached
4	1.2×10^3	0.02	1.1×10^6	1.2
5	2.5×10^3	0.05	2.2×10^6	2.6
6	NA	NA	8.3×10^5	1.2
7	NA	NA	NC*	NC

*Not calculated due to the short duration of Stage 7.

Experiment 2

Since the portion of Experiment 1 measuring detachment (Stages 4 and 5) was inconclusive due to low MS2 concentrations, a second experiment was conducted. In an effort to increase the resolution of MS2 concentrations during the portion of the study where detachment rates are calculated, the injection concentration was increased to 2.68 x 10^4 PFU/ml for Experiment 2. Experiment 2 bromide and MS2 concentrations are plotted against the cumulative number of pore volumes in Figure 5. In Stage 1, the MS2 and bromide breakthrough curves were very similar in shape and position. Bromide spikes were first detected in Stages 1 and 7 at approximately 0.3 and 1.1 PV, respectively, and they peaked after 1.9 PV in Stage 1 and 2.7 PV in Stage 7. The average flow velocity within the column at each pumping rate was calculated using the time required for 50% of the injected bromide concentration to be reached. Average flow velocities for Experiment 2 are provided in Table 2.

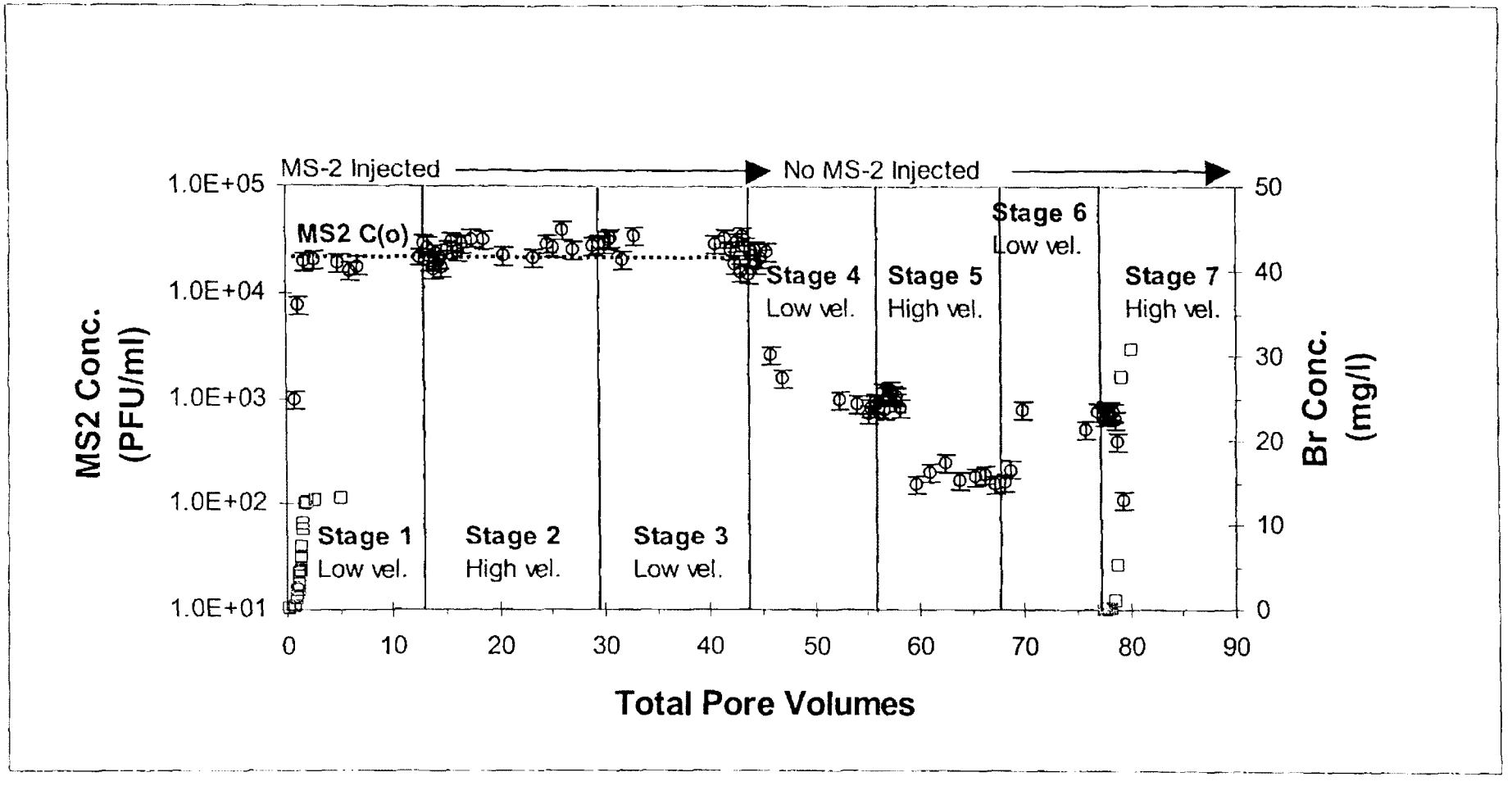

Figure 5. Bromide (□) and MS2 (o) concentrations over total pore volumes for Stages 1-7 of Experiment 2.

The injected MS2 is presumed to have saturated the available binding sites within the column after approximately 12.5 PV. MS2 effluent concentrations were generally equivalent to the injection concentration (within the measurement error) from 12.5 - 45 PV. As a result, Stages 1-3 of Experiment 2 do not provide information on the affect of flow velocity on MS2 transport, however, these stages served to expose the column to the two flow rates during continuous MS2 injection. For this reason, the results and discussion of Experiment 2 will be limited to Stages 4-7. Stages 4-7 were designed to investigate the response of MS2 attached within the column matrix to two different flow velocities.

At the conclusion of Stage 3 (45 total PV), when the injectate was changed over to a virus-free solution, MS2 concentrations decreased rapidly from C_o to 1.6×10^3 PFU/ml after 1.6 PV. The concentrations for the remainder of Stage 4 decreased at a less rapid rate. After the column was subjected to one pore volume at the high flow velocity during Stages 5 and 7, MS2 concentrations rapidly decreased and then stabilized after approximately 2 PV. When the flow velocity was decreased at 68 total PV in Stage 6, MS2 concentrations rapidly increased from 1.6×10^2 PFU/ml to 8.0×10^2 PFU/ml within 2 PV and then remained steadier.

Mass Balance

Table 5 summarizes the MS2 mass distribution over a one-hour time interval during continuous MS2-free injection. The estimated number of MS2 that detached over the time interval was calculated as described for Experiment 1.

Discussion

MS2 Attachment

The data from Stages 1-3 of Experiment 1 relate to net MS2 attachment. As shown in Figure 3, changes in flow velocity had an immediate affect on MS2 effluent concentrations. Figure 4 also illustrates the direct relationship between flow velocity and MS2's mass distribution. In Experiment 1, as the flow velocity increased by nearly one order of magnitude from Stage 1 to Stage 2, the net attachment rate decreased by 6.0 x 10^4 PFU/PV. Similarly, as flow velocity decreased by the same magnitude from Stage 2 to Stage 3, the net attachment rate increased by 4.0 x 10^4 PFU/PV. Since velocity was isolated as the only variable in the column experiment, the trends in MS2 behavior in response to each flow velocity must be a function of either the time MS2 had to interact with the porous media or the physical flow velocity.

If MS2 attached to the porous media at a constant rate relative to time, then in a given amount of time, a constant number of MS2 would be retained within the column regardless of the flow velocity. Table 4 demonstrates that nearly ten times the number of MS2 attached during the high velocity stage (Stage 2) than during the low velocity stages (Stages 1 and 3). Therefore, MS2 does not attach at a constant rate relative to time. Although nearly ten times the number of MS2 attached to the porous media at the high velocity, the column was exposed to over ten times the number of MS2 over the two-hour period. As shown in Table 4, the lowest percentage of attached MS2 occurred at the high

flow velocity. Since MS2 does not appear to attach at a constant rate relative to time, the physical flow velocity must have caused the different MS2 attachment trends observed in the data at the low and high velocities.

To further understand the affect of the physical flow velocity on MS2 attachment, the collision efficiency factor was calculated. The higher the collision efficiency value, the greater the number of collisions that result in MS2 attachment. As shown in Table 6, MS2 more efficiently attaches to sand grains at the low velocity (Stage 1). This supports the attachment trends observed in the data provided in Table 5. Perhaps, the different attachment rates observed at the low and high velocities relates to the number of binding sites exposed to flow at each velocity.

Table 6. Collision Efficiencies for Experiment 1.

Stage	Collision Efficiency
1	0.069
2	0.055

MS2 Detachment

The data from Stages 4 and 5 of Experiment 1 and Stages 4-7 of Experiment 2 relate to net MS2 detachment. Table 5 summarizes the MS2 mass balance over a one-hour period under steady state conditions. The percent of MS2 detached at the high velocities of Experiments 1 and 2 are approximately twice as great as the percent of MS2 detached at the low velocities (Table 5), respectively. Considering that in the one-hour period, the column was exposed to approximately ten times the amount of flow at the high velocity, this is not a substantial increase in detachment rates. This suggests that

velocity may not be the overriding factor dictating MS2 detachment. Rather, MS2 detachment may be predominantly a function of the time MS2 is exposed to flow.

The detachment rate also appears to be concentration dependent. The mass of MS2 retained in the Experiment 2 column was approximately sixty times greater than the mass retained in the Experiment 1 column. The percent of MS2 purged from the Experiment 2 column in a given time interval was approximately twenty times greater than the percent of MS2 purged from the Experiment 1 column (Table 5). Consequently, the data implies that the greater the source concentration, the greater the detachment rate.

Comparison of Attachment Rates and Detachment Rates

Table 7 summarizes the attachment and detachment rates calculated using the number of MS2 retained within, or purged from, the column over a given amount of time. The attachment portion of Table 7 identifies that 65% to 100% of the MS2 injected into the column were attached to the porous media under steady state conditions. This is contrasted with the percentages of MS2 that detached from the Experiment 1 and 2 columns under steady state conditions. The rates that MS2 attached within the column are substantially greater than the rates MS2 was purged from the column.

Table 7. MS2 attachment rates vs. detachment rates.

	Stage	Exp. 1	Exp. 2
Attachment Rates (%)	1	100	NA
	2	65	NA
	3	88	NA
Detachment Rates (%)	4	0.02	1.2
	5	0.05	2.6
	6	NA	1.2
	7	NA	NA

Conclusion

It is well established in the literature that chemical perturbations of ground water systems, such as changes in ionic strength, organic matter, and pH, have dramatic influences on MS2 transport behavior. Bales et al. (1993) observed an increase in MS2 concentration of several orders of magnitude when a spike of 2.5% beef extract in 10^{-3} M sodium phosphate was added to a column at pH 7. In another column experiment, Bales et al. (1991) increased the effluent concentration of PRD-1 three orders of magnitude by increasing the injectate pH from 5.5 to 7.0. Flow rate increases applied during continuous injection of a constant virus concentration in this study produced similar results as those observed from these chemical perturbations. MS2 effluent concentrations increased by nearly 2 orders of magnitude after a one $\log_{10}$ increase in flow velocity.

This study suggests flow velocity and virus attachment are inversely related. Lower flow velocities result in more rapid virus attachment. This relationship supports the findings of several previous studies (Smith et al., 1985; Wollum and Cassel, 1978; Tan et al., 1994). The degree of virus attachment appears to be a function of the number of binding sites exposed to flow at the different velocities. The flow velocities applied in this study were greater than those used in all previous column studies using granular material. Consequently, this study expanded the velocity range in which this inverse relationship between flow velocity and virus attachment was observed.

The results from this study also suggest that virus detachment is largely a function of the time MS2 is exposed to flow and the source concentration. Flow velocity did not appear to greatly influence the detachment rates observed in both experiments.

Results obtained from Experiment 1 indicate that attachment rates are significantly greater than detachment rates. This supports the findings of several researchers (DeBorde et al., 1999; Ryan et al. 1998; Pieper et al., 1997; Bales et al., 1991). These researchers observed prolonged tailing of virus breakthrough curves when chemical and physical parameters remained constant. Bales et al. (1991) concluded that time scales for attachment are on the order of hours, whereas time scales for detachment are on the order of days.

Conclusions from this study should be considered when formulating governing equations to predict virus transport. The recently proposed Ground Water Rule encourages the use of models to predict the flow distance required for natural disinfection to occur. To accomplish this, governing equations must be flexible to allow different attachment rates, based on ground water velocity. Therefore, a microorganism attachment rate observed at one site may be inappropriate to use at another site where there is a different ground water velocity. This adds another layer of complexity to predicting microorganism transport. To a lesser extent, these predictive models should consider the source concentration when assigning detachment rates. Since attachment rates are much greater than detachment rates, it is of primary importance to assign accurate pathogen attachment rates in predictive models. It is of lesser importance to ensure accurate detachment rates.

Conclusions from this study may also be useful for establishing emergency response strategies for ground water recently impacted by virus. If, for example, a sewage line ruptures and releases pathogens to ground water, it would be prudent to

artificially increase ground water velocity by pumping nearby remediation wells. This strategy would mitigate the pathogen mass that becomes attached within the aquifer. After some time has elapsed since the incident, and the pathogens have had enough time to attach to aquifer sediments, results from this study suggest that the ground water velocity does not greatly increase pathogen detachment. As a result, the continued, long-term pumping of nearby remediation wells would not be an effective remediation strategy once initial attachment has occurred.

Literature Cited

Alhajjar, B. J.; Stamer S.L.; Cliver, D.O.; Harkin, J.M. *Water Research.* **1988.**22, 907-915.

Bales, R.C.; Gerba, C.P.; Grondin, G.H.; Jensen, S.L. *Applied and Environmental Microbiology.* **1989.** 55, 2061-2067.

Bales, R.C.; Hinkle, S.R.; Kroeger, T.W.; Stocking, K.; Gerba, C.P. *Environmental Science and Technology.* **1991.** 25, 2088-2095.

Bales, R.C.; Li, S.; Maguire, K.M.; Yahya, M.T.; Gerba, C.P. *Water Resources Research.* **1993.** 29, 957-963.

Bales, R.C.; Li, S.; Maguire, K.M.; Yahya, M.T.; Gerba, C.P.; Harvey, R.W. *Ground Water.* **1995.** 33. 653-661.

Bales, R.C.; Li, S.; Yeh, J.T.C.; Lenczewski, M.E.; Gerba, C.P. *Water Resources Research.* **1997.** 33. 639-648.

Cairncross, S. *Water Sanitation Dis.* 1992. 9.

Chrysikopoulos, C.V.; Sim, Y. *Journal of Hydrology* (Amsterdam). **1996.** 185. 199-219.

Cole, B.E.; Sillman, S.E. *Ground Water.* **1997.** 35. 92-98.

DeBorde, D.C.; Woessner, W.W.; Lauerman, B.; Ball, P.N. *Ground Water.* **1998.** 36. 825-834.

DeBorde, D.C.; Woessner, W.W.; Kiley, Q.T.; Ball, P. *Water Research.* **1999.** 33. 2229-2238.

Gerba, C.P.; Rose, J.B. *Drinking Water Microbiology*; Springer-Verlag: New York, 1990; pp.380-396.

Harton, A.D.; McKay, L.D.; Wilson, G.V. Submitted to *Water Resources Research.* **1998.**

Harvey, R.W. and Garabedian S.P. *Environmental Science and Technology.* **1991.** 25. 178-185.

Hinsby, K. *Ground Water.* **1996.** 34. 1065-1075.

Huber, M.S.; Gerba, C.P.; Abbaszadegan, M.; Robinson, J.A.; Bradford, S.M. *Environmental Science and Technology.* **1994.** 28. 1767-1772.

Koltermann, C.E.; Gorelick, S.M. *Water Resources Research.* **1996.** 32. 2617-2658.

Lance, J.C.; Gerba, C.P. *Journal of Environmental Quality.* **1980.** 9. 31-34.

Macler, B.A. *Ground Water Monitoring and Remediation.* **1995.** 77-84.

Penrod, S.L.; Olson,T.M.; Grant, S.B. *Langmuir.* **1996.** 12. 5576-5587.

Pieper, A.P.; Ryan, J.N.; Harvey, R.W.; Amy, G.L.; Illangasekare, T.H.; Metge, D.W. *Environmental Science and Technology.* **1997.** 31. 1163-1170.

Rossi, P.; De Carvalho-Dill, A.; Muller, I.; Aragno, M. *Environmental Geology.* **1994.** 23. 192-200.

Ryan, J.N.; Elnachem, E.; Ard, R.A.; Harvey, R.W.; Johnson, P.R. *Environmental Science and Technology.* **1998.** 33. 63-73.

Skilton, H. and Wheeler, D. *Journal of Applied Bacteriology.* **1988.** 65. 387-395.

Smith, M.S.; Thomas, G.W.; White, R.E.; Ritonga, D. *Journal of Environmental Quality.* **1985.** 14. 87-91.

Tan, Y.; Gannon, J.T.; Baveye, P.; Alexander, M. *Water Resources Research.* **1994.** 30. 3243-3252.

VanDuin, J. In *The Bacteriophages*, 1st ed.; Calender,R., Ed.; Plenum Press: New York, **1988**; 1, 117-167.

Wang, D.; Gerba, C.P.; Lance, J.C. *Applied and Environmental Microbiology.* **1981.** 42. 83-88.

Woessner, W.W.; Troy, T.; Ball, P.; DeBorde, D.C. **1998.** Proceedings of Source water protection International 98, Dallas, Texas, April 28-30, National Water Research Institute, p. 167-174.

Wollum, A.G. II; Cassel, D.K. *Soil Science Society.* **1978.** 42. 72-76.

Yahya, M.T.; Galsomies, L.; Gerba, C.P.; Bales, R.C. *Water Science Technology.* **1993.** 27. 409-412.

Yan, J.; Yates, M.V.; Thompson, S.S.; Jury, W.A. *Environmental Science and Technology.* **1997.** 31. 548-555.

Yates, M.V.; Gerba, C.P.; Kelley, L.M. *Applied and Environmental Microbiology.* **1985.** 49. 778-781.

Yates, M.V.; Yates, S.R. *Water Research.* **1987.** 21. 1119-1125.

Zerda, K.S.; Gerba, C.P.; Hou, K.C.; Goyal, S.M. *Applied and Environmental Microbiology.* **1985.** 49. 91-95.

Appendix A

Bromide Breakthrough Curves

A bromide tracer was injected at the beginning of Stages 1 and 2 of Experiment 1 and at the beginning of Stages 1 and 7 of Experiment 2. The 50% C_o point was used on each plot of concentration and time (Figures A-1 through A-4) to estimate the mean transport velocity during a given stage. Table A-1 lists the number of hours to attain 50% C_o (critical time) for each stage. In Experiment 1 the critical time for Stage 1 (low flow rate) was 2.19 hours and the critical time for Stage 2 (high flow rate) was 0.25 hours. Similar results were found from the Experiment 2 bromide curves. The critical time for Stage 1 (low flow rate) of Experiment 2 was 2.45 hours and the critical PV for Stage 7 (high flow rate) was 0.28 hours.

Table A-1. Bromide tracer flow velocities.

	Critical Time (hours)	Flow Velocity (m/d)
Stage 1, Exp. 1	2.19	14
Stage 2, Exp. 1	0.25	118
Stage 1, Exp. 2	2.45	12
Stage 7, Exp. 2	0.28	105

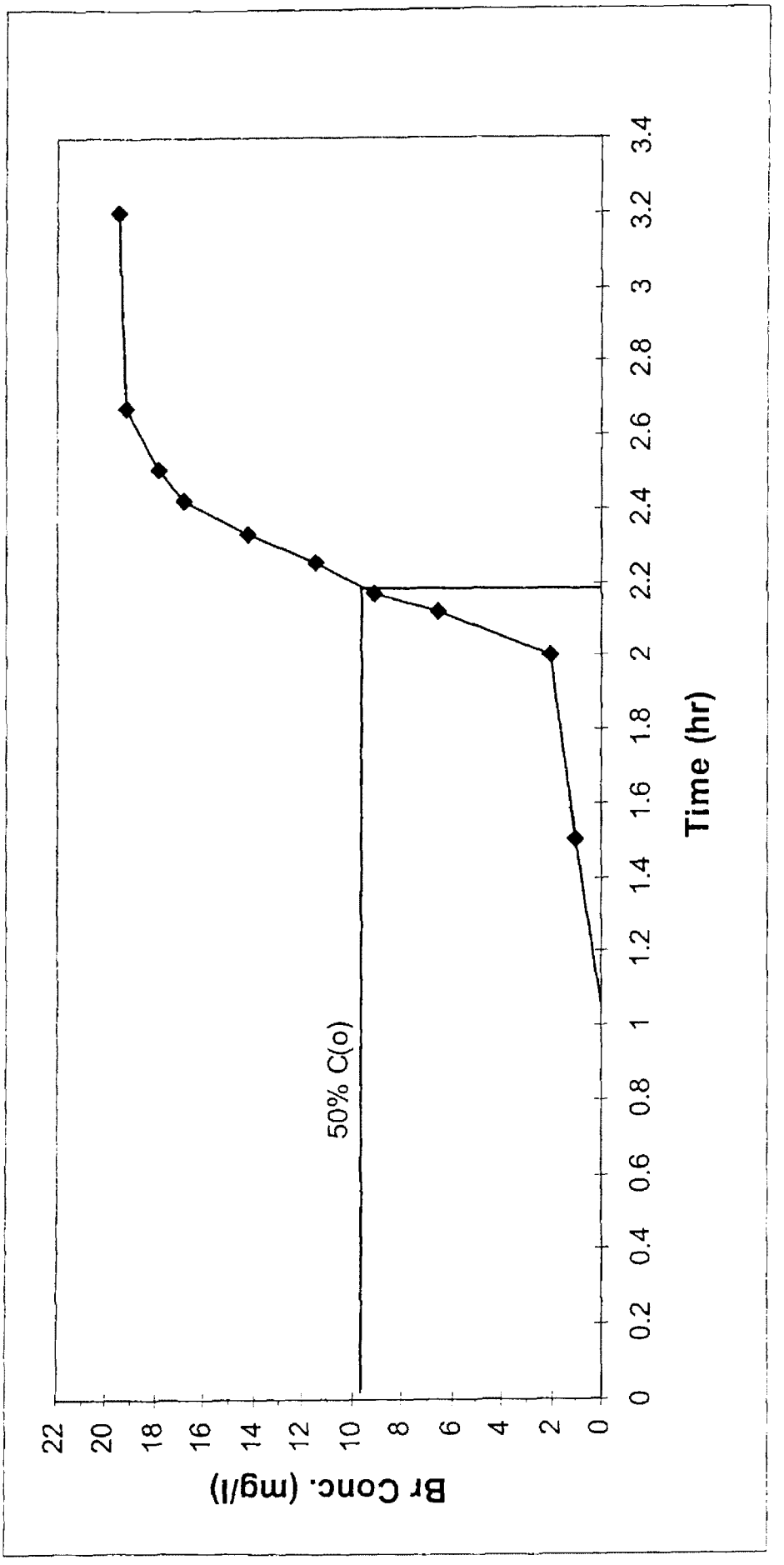

Figure A-1. Bromide concentration over time for Stage 1 of Experiment 1.

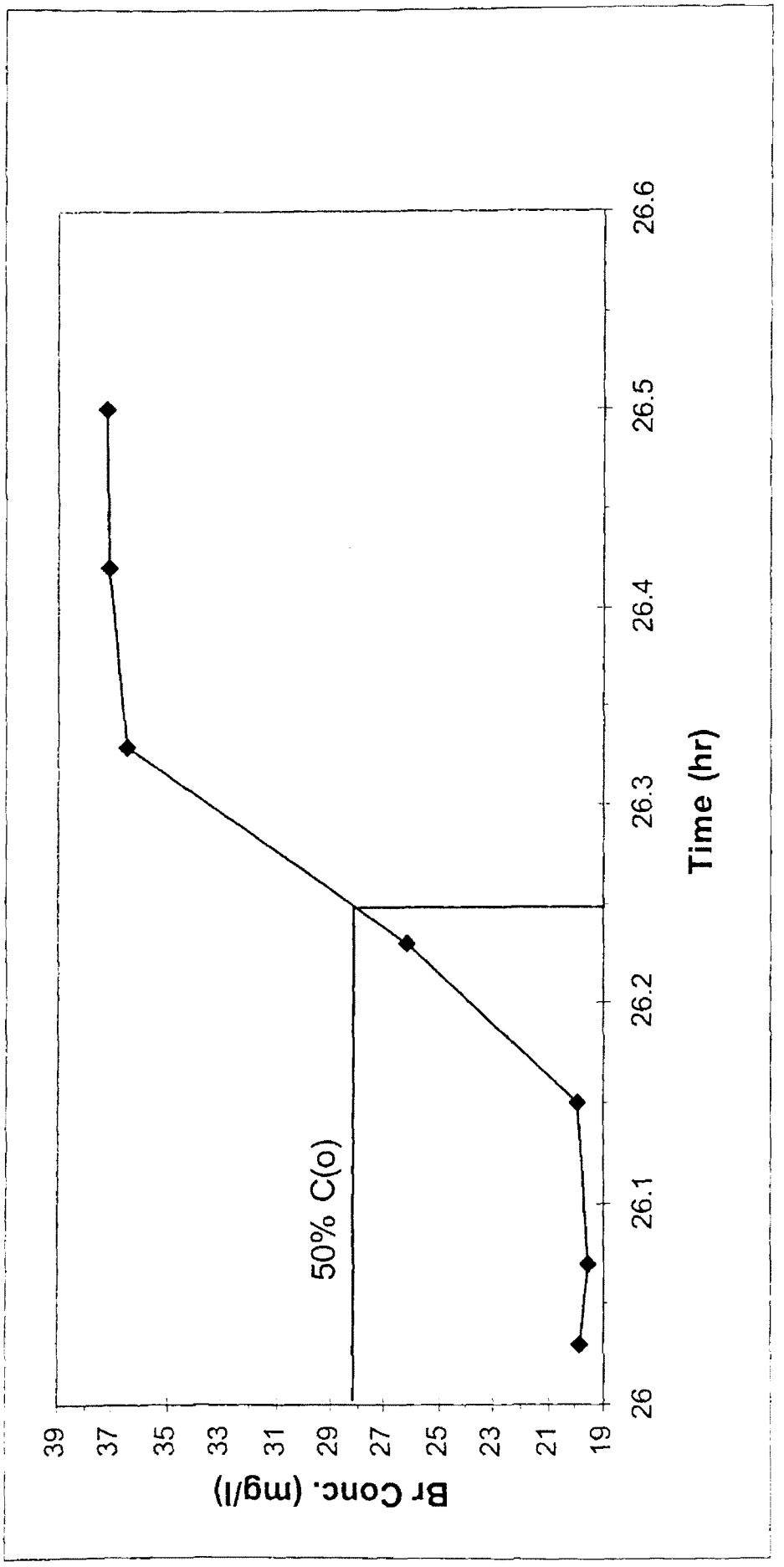

Figure A-2. Bromide concentration over time for Stage 2 of Experiment 1.

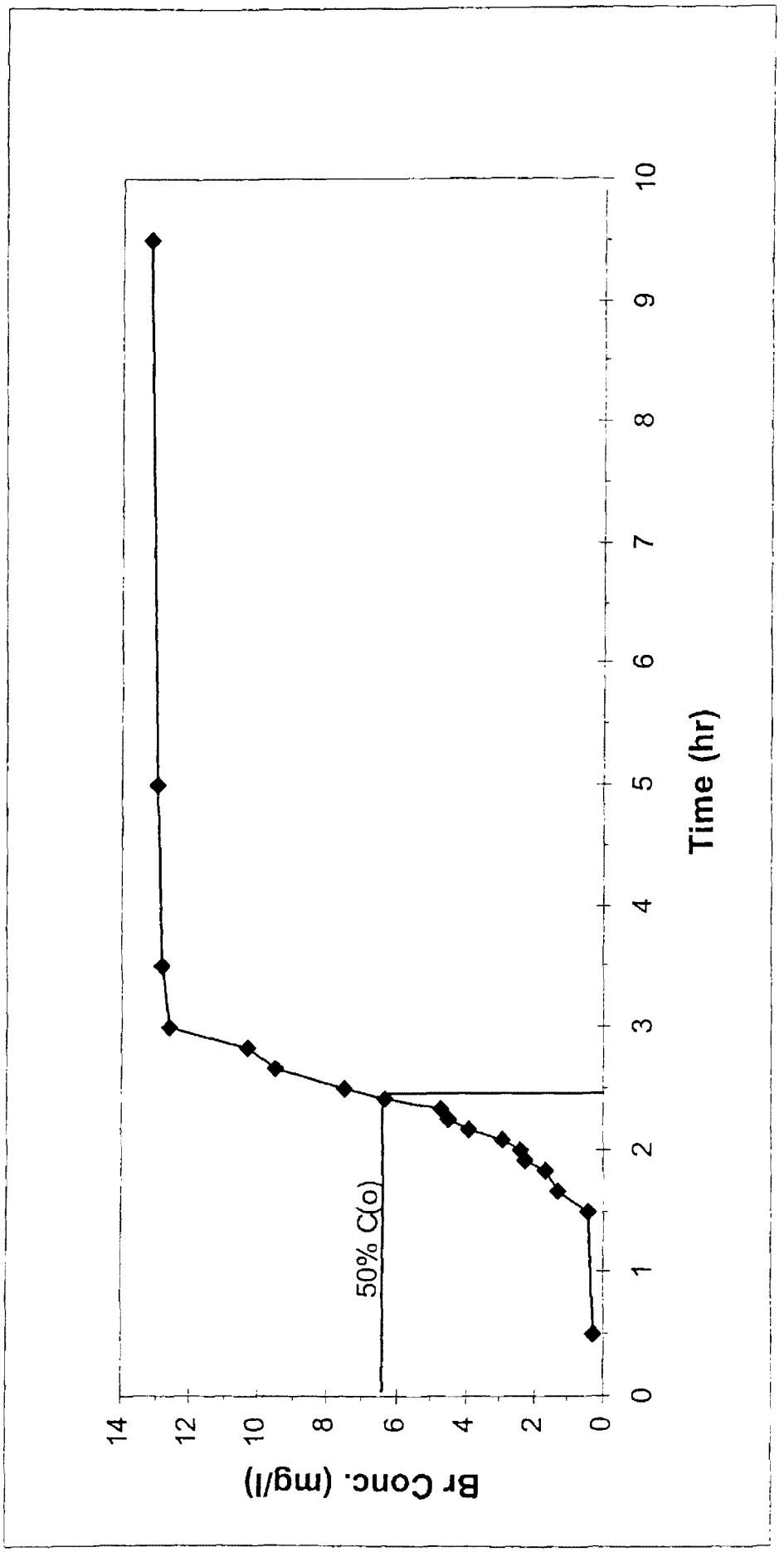

Figure A-3. Bromide concentration over time for Stage 1 of Experiment 2.

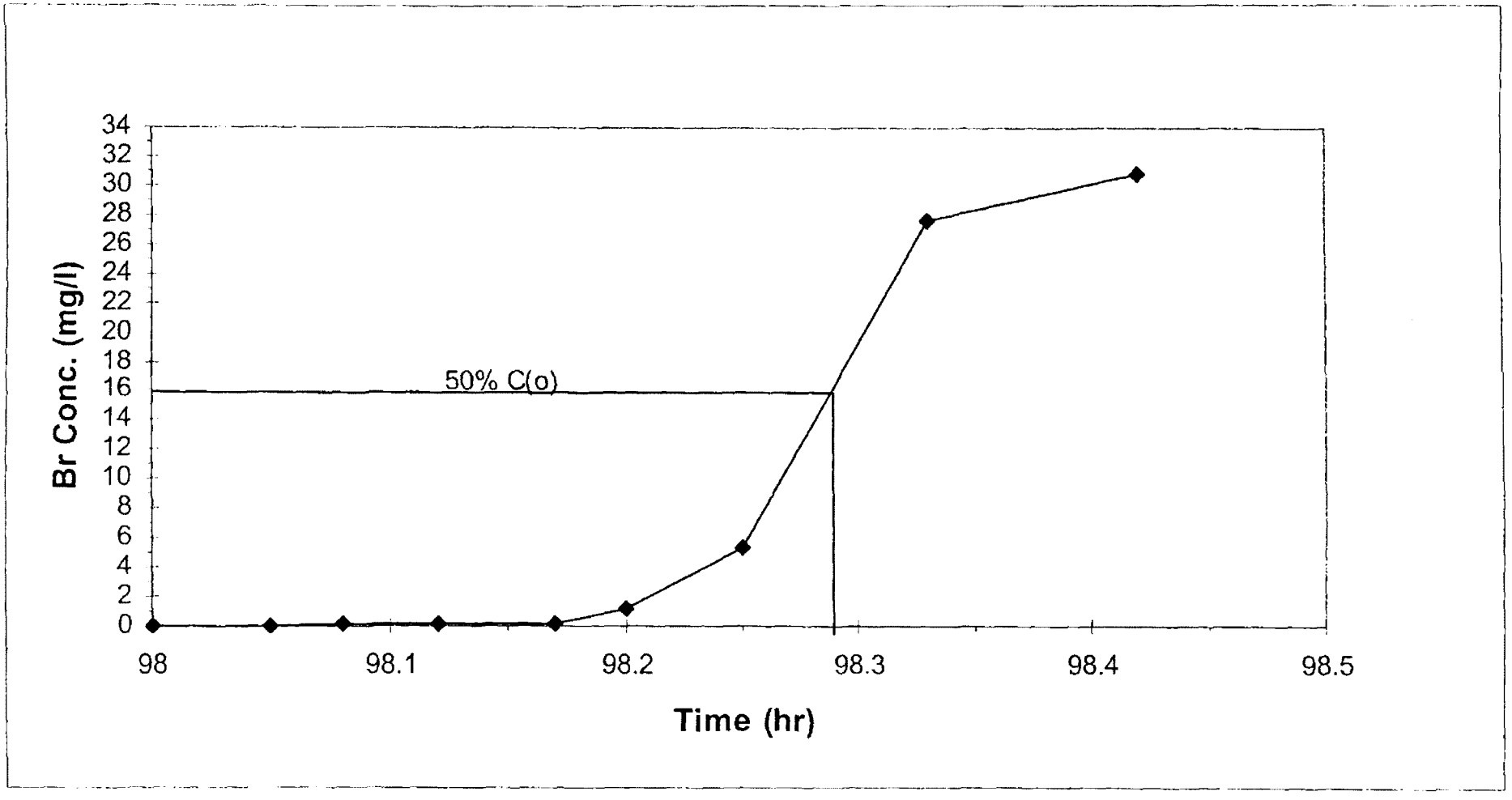

Figure A-4. Bromide concentration over time for Stage 7 of Experiment 2.

Appendix B

Mass Balance Estimation

The mass of MS2 recovered from the columns over the duration of Experiments 1 and 2 were estimated by integrating the area of the MS2 curve shown in Figures B-1 and B-2, respectively, using discrete time steps. The cumulative mass recovered during the experiment is comprised of both the mass that did not attach within the column and the mass that attached, and then detached into the aqueous phase and flowed out of the column. The mass of MS2 injected into the column was calculated by multiplying the mean injection concentration by the volume of injectate used during Stages 1-3 of each experiment. This value was adjusted to account for the travel time through the column. This was accomplished by assuming that the MS2 breakthrough curves in Stages 1 and 2 were of similar shape and position to the bromide breakthrough curves in Stage 1 and 2. This correlation between virus and bromide breakthrough curves has been observed in other column studies (DeBorde et al., 1998; Bales et al., 1995). By accounting for MS2's transit time through the column, the cumulative mass recovered can be subtracted from the cumulative mass injected to estimate the cumulative mass retained within the column at any given time.

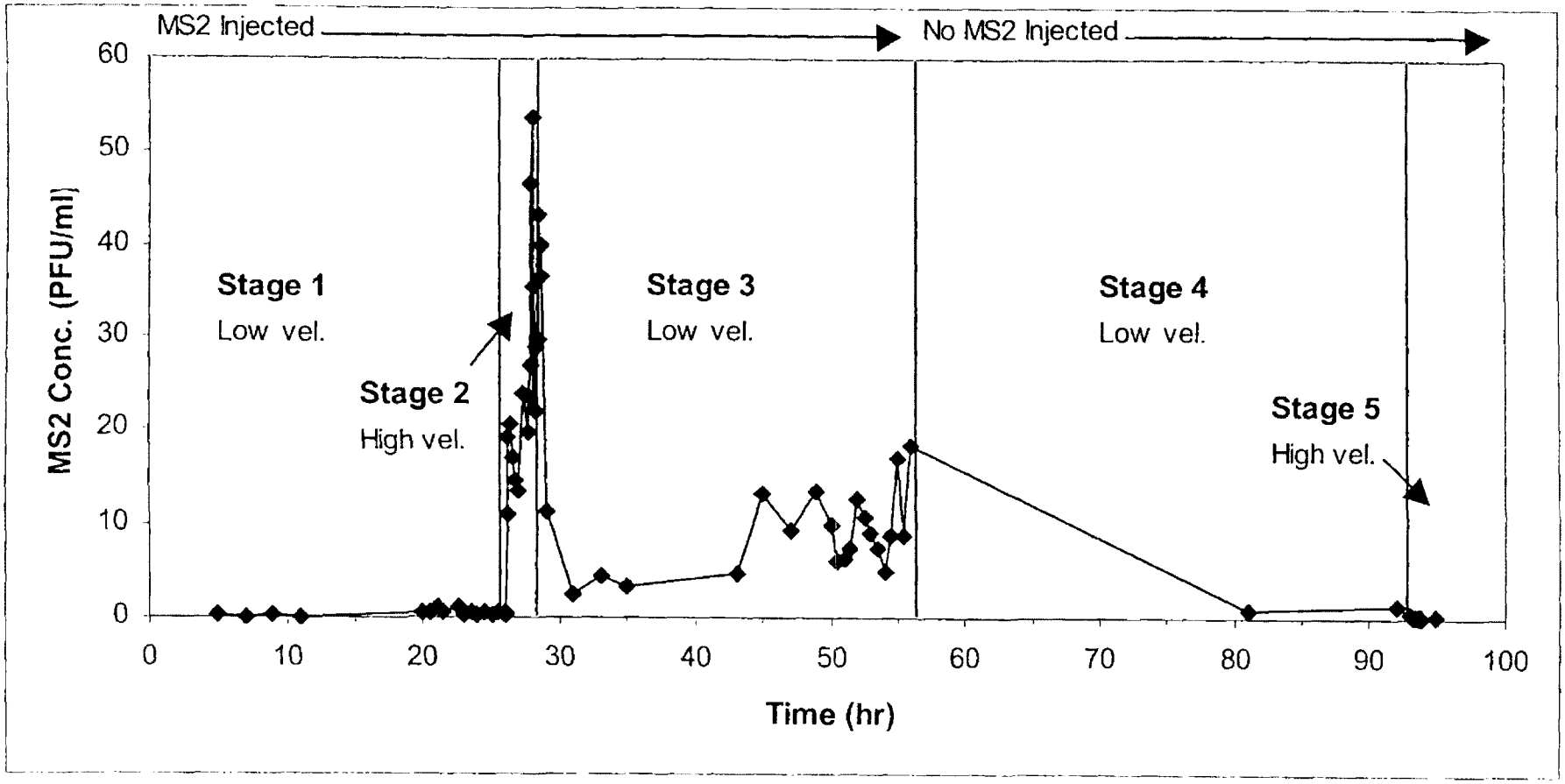

Figure B-1. MS2 concentration over time for Experiment 1.

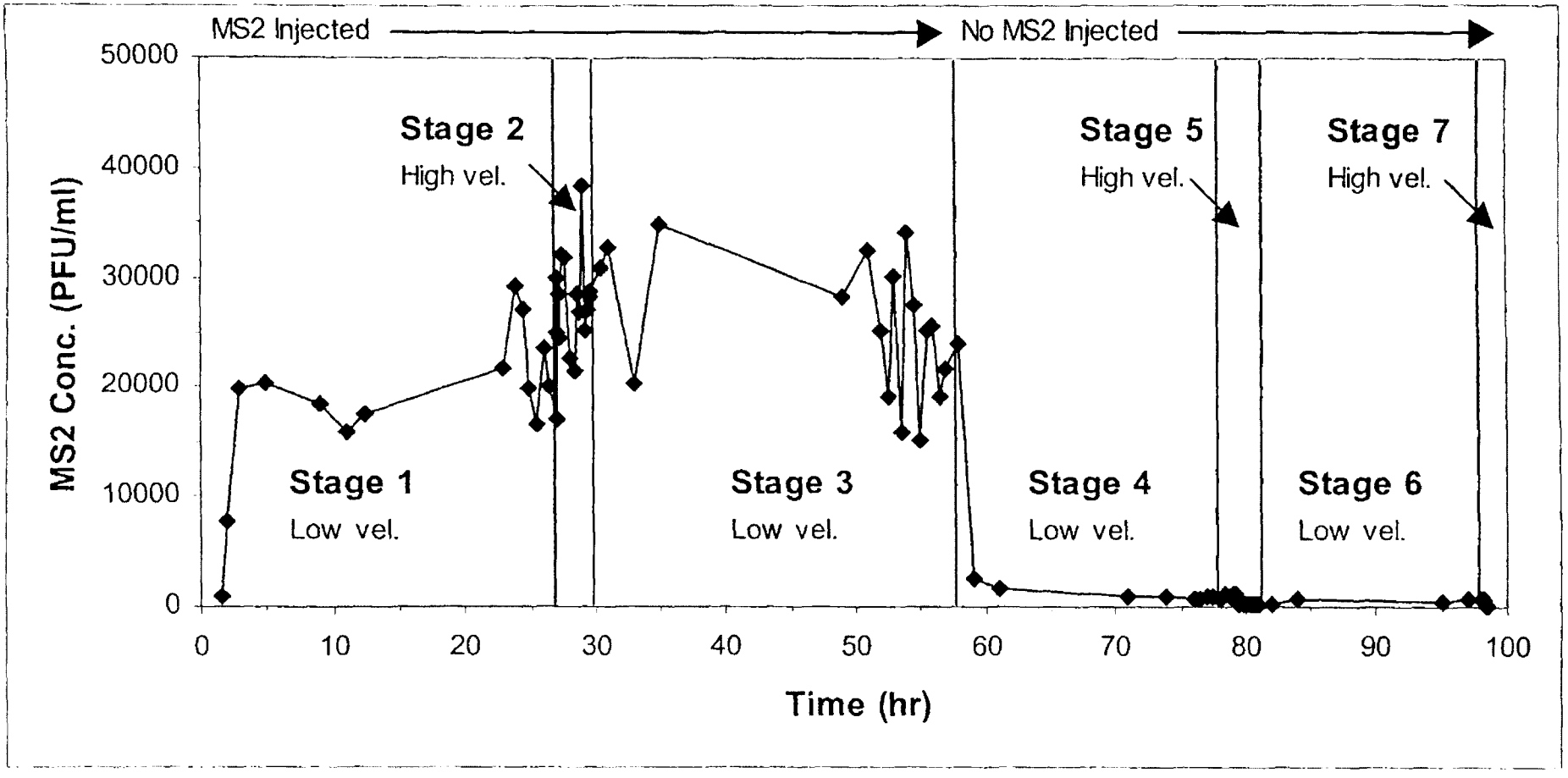

Figure B-2. MS2 concentration over time for Experiment 2.

Appendix C

Preliminary Experiments

Two preliminary, up-flow column experiments were conducted to determine if the desired experimental procedure could be logistically attained by using the proposed methods and column structure. The column materials, injectate, sampling procedure, and analysis methods used in the main study were generally used in both preliminary experiments.

Preliminary Experiment 1

A PVC column measuring 1.23 m in length and 7.62 cm inner diameter with standpipe piezometers and influent and effluent Tygon tubing was constructed and gravity filled with fine (1-2mm) gravel obtained from a local gravel yard. The column was placed in a room with a controlled temperature of 14 °C and site water was injected through the bottom of the column at 20 ml/min with a peristaltic pump. After the column sediment was saturated, a porosity value of 0.37 was calculated. The column was conditioned for 3 PV at the same flow rate. Site water spiked with 1.46×10^5 PFU/ml MS2 and 49 mg/l NaBr was homogenized and then injected into the column throughout the experiment. Preliminary Experiment 1 included three stages with alternating flow rates. Stages 1 and 3 were conducted at a flow rate of 20 ml/min and Stage 2 was conducted at 200 ml/min. MS2 and bromide samples were periodically collected from the effluent and replicate C_o samples were collected directly from the injectate reservoir. MS2 samples were collected in sterile 15 ml glass vials and immediately placed on ice

and bromide samples were collected in 50 ml sterile polypropylene containers. MS2 and bromide samples were analyzed as stated in the main study.

Figure C-1 shows the MS2 and bromide concentrations plotted against PV. MS2 was first detected after 0.66 PV and it increased to 8.47 x 10^4 PFU/ml (58% of C_o) after 1.44 PV and then decreased to 4.66 x 10^4 PFU/ml after 1.89 PV. MS2 concentrations generally varied within this range for the remainder of the experiment.

Although MS2 transport did not appear to be influenced by flow rate, Preliminary Experiment 1 allowed the researcher to practice the sampling methodology and analysis and it also confirmed the integrity of the column set up and procedure.

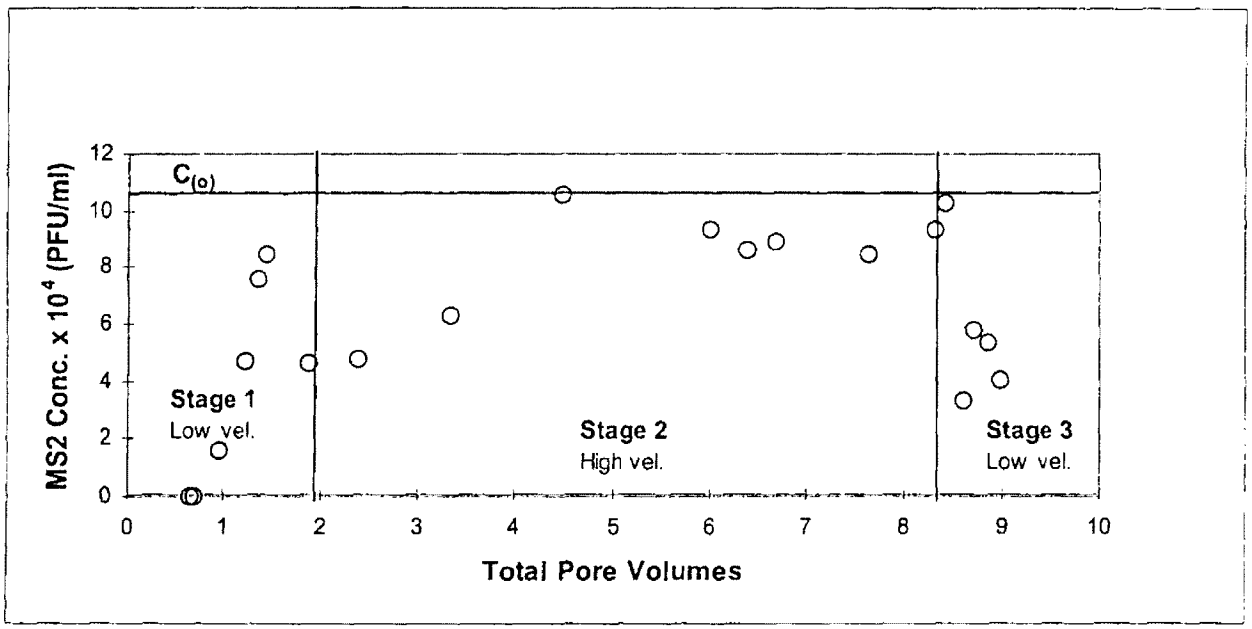

Figure C-1. MS2 concentration (O) over total pore volumes for Preliminary Experiment 1.

Preliminary Experiment 2

Based on the success of Preliminary Experiment 1, a second preliminary experiment was performed with finer column sediment in an effort to better retain MS2. Preliminary Experiment 2 was conducted using the same methodology as Experiment 1, with three notable exceptions. First, 7.0 mM of KNO_3 was added to the injectate to increase the ionic strength of the solution to aid in bromide analysis; second, the experiment only included three stages; and third, each of the three stages only lasted approximately 5 PV.

As shown in Figure C-2, MS2 was first detected in Stage 1 at 1.9 PV and concentrations gradually increased until the conclusion of Stage 2. In the beginning of Stage 3 MS2 concentrations decreased, but as Stage 3 continued, concentrations increased to levels observed near the conclusion of Stage 2. No obvious trend between flow rate and MS2 concentrations was observed in Preliminary Experiment 2, however, the experiment duration appeared to be too brief to detect potential trends.

Based on Preliminary Experiment 2 it was decided to increase the duration of the experiment to allow MS2 concentrations to equilibrate and to omit the complicating factor of added ionic strength. By the completion of the two preliminary experiments, an appropriate sampling methodology and sampling schedule was determined for the initiation of Experiment 1.

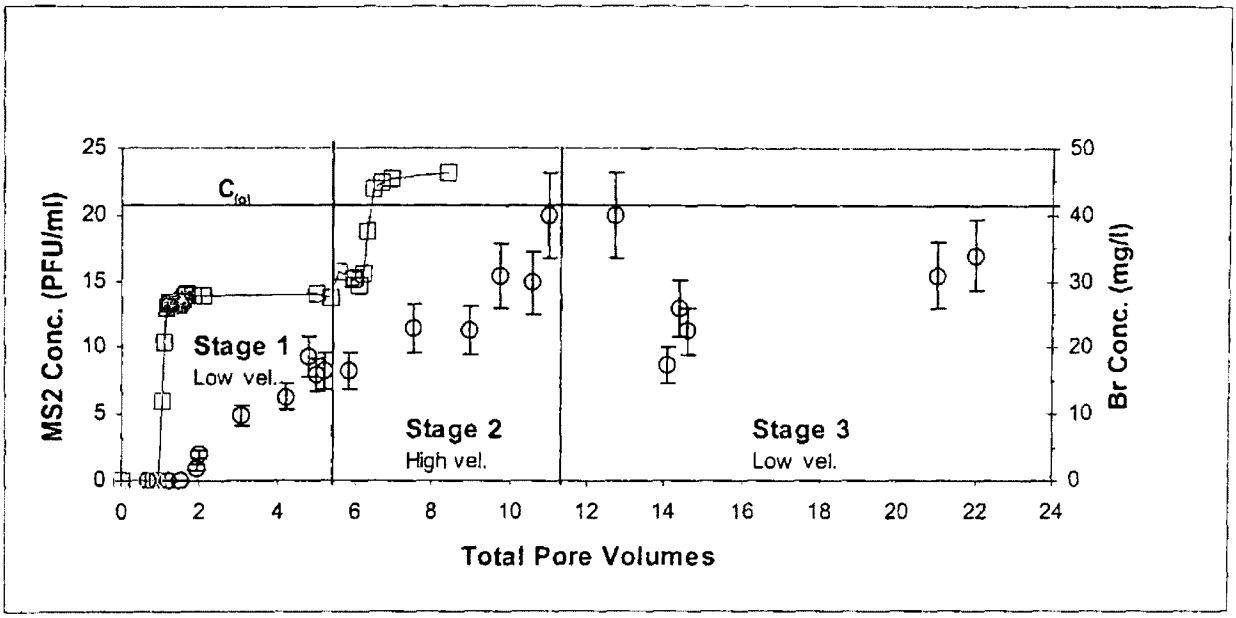

Figure C-2. MS2 concentration (o) and bromide concentration (□) over total pore volumes for Preliminary Experiment 2.

Appendix D

Hydraulic Conductivity Calculations

Hydraulic conductivity values for the two columns were calculated using two independent methods. The first method was based on the dimensions of the column (length (L), and area (A)), discharge (Q), and the observed hydraulic gradient (I). According to the following formula, hydraulic conductivity was calculated to be 43 and 52 m/d for Experiments 1 and 2, respectively.

$$K = Q/(AI)$$

The second method used the column porosity (n), the observed hydraulic gradient (I), and the mean transport velocity (v) within the column, which was estimated from the 50% C_o arrival time of the bromide tracer. According to the following formula, hydraulic conductivity was calculated to be 36 and 39 m/d for Experiments 1 and 2, respectively.

$$K = (vn)/I$$

All calculations were performed using the data collected at the low flow rate since the hydraulic gradient for the high flow rate could not be attained using the methods described in the text.

Appendix E

Experiment 1 Data

Bromide tracer data for Stages 1 and 2 of Experiment 1.

time (hr)	Approx # of PVs	Br Conc. (mg/l)
1.5	0.754286	1.04
2	1.025714	2.06
2.12	1.094286	6.55
2.17	1.122857	9.19
2.25	1.168571	11.5
2.33	1.214286	14.3
2.42	1.265714	16.9
2.5	1.311429	17.9
2.67	1.408571	19.2
3.2	1.711429	19.5
10	5.597143	19.9
20.5	11.33286	20.3
26.03	13.75514	19.8
26.07	13.962	19.6
26.15	14.37571	19.9
26.23	14.78943	26.2
26.33	15.30657	36.5
26.42	15.772	37.1
26.5	16.18571	37.2

jugs	mg/l
1 hr-1	19.8
1 hr-1	18.3
1hr-2	19.6
26hr-2	35.3
26hr-2	36.5
26hr-1	37.4
26hr-1	37
avg	36.55
stdev	0.911043
%RSD	2.492595

MS2 data for Experiment 1.

			Cumulative					
	Elapsed		Approx. # of				Conc.	
Sample	Time (hr)	dilution	PVs	Plate 1	Plate 2	Total Counts	PFU/ml	Means
Jug (1 hr)-1	1	0.1	0.5	32	29	61	67.1	52.8
Jug (1 hr)-2		0.1		21	39	60	66	
Jug (1 hr)-3		0.1		19	26	45	49.5	
Jug (1 hr)-4		0.1		13	13	26	28.6	
Jug (20 hr)-1	20	0.1	10.9	20	34	54	59.4	64.1
Jug (20 hr)-2		0.1		47	55	102	112.2	
Jug (20 hr)-3		0.1		14	11	25	27.5	
Jug (20 hr)-4		0.1		24	28	52	57.2	
Jug (43 hr)-1	43	0.1	36.3	41	33	74	81.4	80.3
Jug (43 hr)-2		0.1		27	30	57	62.7	
Jug (43 hr)-3		0.1		41	39	80	88	
Jug (43 hr)-4		0.1		44	37	81	89.1	
Jug (56hr)-1	56	0.1	43.3	53	46	99	108.9	91.9
Jug (56hr)-2		0.1		47	40	87	95.7	
Jug (56hr)-3		0.1		28	35	63	69.3	
Jug (56hr)-4		0.1		38	47	85	93.5	
dummy value	1		0.5					0.0
5	5	0.5	2.6	1	0	1	0.22	0.2
7	7	0.5	3.8	0	0	0	0	0.0
9	9	0.5	4.9	1	0	1	0.22	0.2
11.0-1	11	1	5.9	2	2	4	0.44	0.1
11.0-2		1		0	1	1	0.11	
11.0-3		1		0	0	0	0	
11.0-4		1		0	0	0	0	
20	20	0.5	10.5	2	1	3	0.66	0.7
20.5	20.5	0.5	10.8	2	0	2	0.44	0.4
21	21	0.5	11.0	5	0	5	1.1	1.1

	21.5	21.5	0.5	11.3	2	1	3	0.66	0.7
	22.5	22.5	0.5	11.8	3	2	5	1.1	1.1
	23	23	0.5	12.1	1	0	1	0.22	0.2
	23.5	23.5	0.5	12.3	0	3	3	0.66	0.7
24-1		24	1	12.6	2	2	4	0.44	0.2
24-2			1		0	2	2	0.22	
24-3			1		1	0	1	0.11	
24-4			1		0	1	1	0.11	
	24.5	24.5	0.5	12.8	0	2	2	0.44	0.4
25-1		25	1	13.1	2	2	4	0.44	0.3
25-2			1		0	2	2	0.22	
25-3			1		3	1	4	0.44	
25-4			1		0	1	1	0.11	
	25.5	25.5	0.5	13.4	1	1	2	0.44	0.4
26-1		26	1	13.6	0	1	1	0.11	0.2
26-2			1		1	0	1	0.11	
26-3			1		1	0	1	0.11	
26-4			1		2	1	3	0.33	
	26.08	26.08	0.5	14.0	2	0	2	0.44	0.4
	26.17	26.17	0.5	14.5	32	18	50	11	11.0
	26.25	26.25	0.5	14.9	46	41	87	19.14	19.1
	26.33	26.33	0.5	15.3	51	43	94	20.68	20.7
	26.5	26.5	0.5	16.2	36	42	78	17.16	17.2
	26.67	26.67	0.5	17.2	34	32	66	14.52	14.5
	27	27	0.5	19.0	32	29	61	13.42	13.4
27.33-1		27.33	0.5	20.9	57	59	116	25.52	23.9
27.33-2			0.5		43	58	101	22.22	
27.33-3			0.5		78	53	131	28.82	
27.33-4			0.5		46	40	86	18.92	
	27.67	27.67	0.5	22.8	46	40	86	19.78	19.8
	27.75	27.75	0.5	23.3	52	56	108	23.76	23.8

	27.83	27.83	0.5	23.7	68	55	123	27.06	27.1
	27.92	27.92	0.5	24.2	103	109	212	46.64	46.6
	28	28	0.5	24.7	118	126	244	53.68	53.7
	28.08	28.08	0.5	25.1	53	48	101	22.22	22.2
	28.17	28.17	0.5	25.6	72	90	162	35.64	35.6
	28.25	28.25	0.5	26.1	47	53	100	22	22.0
28.33-1		28.33	0.5	26.6	67	69	136	29.92	28.8
28.33-2			0.5		45	44	89	19.58	
28.33-3			0.5		51	66	117	25.74	
28.33-4			0.5		85	96	181	39.82	
	28.42	28.42	0.5	27.1	59	76	135	29.7	29.7
28.5-1		28.5	0.5	27.5	111	90	201	44.22	43.2
28.5-2			0.5		98	75	173	38.06	
28.5-3			0.5		89	93	182	40.04	
28.5-4			0.5		121	109	230	50.6	
	28.58	28.58	0.5	28.0	87	80	167	36.74	36.7
28.67-1		28.67	0.5	28.5	84	61	145	31.9	39.9
28.67-2			0.5		78	84	162	35.64	
28.67-3			0.5		81	71	152	33.44	
28.67-4			0.5		132	134	266	58.52	
	29	29	0.5	28.7	32	19	51	11.22	11.2
	31	31	0.5	29.7	7	4	11	2.42	2.4
	33	33	0.5	30.8	12	8	20	4.4	4.4
	35	35	0.5	31.9	6	9	15	3.3	3.3
	43	43	0.5	36.3	13	8	21	4.62	4.6
	45	45	1	37.3	54	65	119	13.09	13.1
	47	47	0.5	38.4	21	21	42	9.24	9.2
49-1		49	0.5	39.5	30	23	53	11.66	13.6
49-2			0.5		34	24	58	12.76	
49-3			0.5		49	31	80	17.6	
49-4			0.5		30	26	56	12.32	

	50	50	0.5	40.1	23	22	45	9.9	9.9
	50.5	50.5	0.5	40.3	17	11	28	6.16	6.2
	51	51	0.5	40.6	18	11	29	6.38	6.4
	51.5	51.5	0.5	40.9	13	21	34	7.48	7.5
	52	52	0.5	41.1	28	29	57	12.54	12.5
	52.5	52.5	0.5	41.4	34	15	49	10.78	10.8
	53	53	0.5	41.7	29	12	41	9.02	9.0
	53.5	53.5	0.5	42.0	13	21	34	7.48	7.5
	54	54	0.5	42.2	12	11	23	5.06	5.1
	54.5	54.5	0.5	42.5	24	16	40	8.8	8.8
	55	55	0.5	42.8	39	38	77	16.94	16.9
	55.5	55.5	0.5	43.1	19	21	40	8.8	8.8
56-1		56	0.5	43.4	35	38	73	16.06	18.5
56-2			0.5		31	43	74	16.28	
56-3			0.5		56	59	115	25.3	
56-4			0.5		38	37	75	16.5	
81-1		81	1	58.1	8 plates	8 plates	25	0.6875	0.9
81-2			1		8 plates	8 plates	28	0.77	
81-3			1		8 plates	8 plates	36	0.99	
81-4			1		8 plates	8 plates	45	1.2375	
92-1		92	1	64.5	8 plates	8 plates	42	1.155	1.3
92-2			1		8 plates	8 plates	82	2.255	
92-3			1		8 plates	8 plates	34	0.935	
92-4			1		8 plates	8 plates	34	0.935	
93-1		93	1	65.1	8 plates	8 plates	17	0.472222	0.6
93-2			1		8 plates	8 plates	25	0.694444	
	93.25	93.25	1	66.5	8 plates	8 plates	14	0.385	0.4
	93.42	93.42	1	67.5	8 plates	8 plates	9	0.2475	0.2
	93.5	93.5	1	67.9	8 plates	8 plates	9	0.2475	0.2
	93.67	93.67	1	68.9	8 plates	8 plates	4	0.11	0.1
93.83-1		93.83	1	69.8	8 plates	8 plates	7	0.1925	0.2

93.83-2			1	8 plates	8 plates	7	0.1925		
93.83-3			1	8 plates	8 plates	8	0.22		
93.83-4			1	8 plates	8 plates	9	0.2475		
	94.83	94.83	1	75.5 8 plates	8 plates	7	0.1925	0.2	

Appendix F

Experiment 2 Data

Bromide tracer data for Stages 1 and 7 of Experiment 2.

Elapsed Time (hr)	Approx. # PVs	Br Conc. (mg/l)
0.5	0.261429	0.33
1.5	0.792857	0.45
1.67	0.8832	1.36
1.83	0.970057	1.71
1.92	1.018914	2.3
2	1.062343	2.4
2.08	1.105771	2.98
2.17	1.154629	3.9
2.25	1.198057	4.47
2.33	1.241486	4.72
2.42	1.290343	6.35
2.5	1.333771	7.5
2.67	1.426057	9.51
2.83	1.512914	10.3
3	1.6052	12.6
3.5	1.876629	12.8
5	2.690914	13
9.5	5.133771	13.2
98	77.5	0
98.05	77.6	0
98.08	77.8	0.178
98.12	78	0.164
98.17	78.13	0.148
98.2	78.5	1.24
98.25	78.8	5.3
98.33	79.2	27.6
98.42	80.1	30.9

jug		
	0.42	12.7
	0.42	13.2
	0.42	13.6
	0.42	13.1
	0.42	13.3
	0.42	12.7
avg		13.1
stdev		0.352136
%RSD		2.688064

jug		
	98.25	30.3
	98.25	31.1
	98	31.3
	98.25	30.4
	98	31.4
avg		30.9
stdev		0.514782
%RSD		1.66596

MS2 data for Experiment 2.

							MS2	
	elapsed		Approx #				conc.	
Sample	time (hr)	dilution	PVs	plate1	plate 2	total	(PFU/ml)	means
Jug(dir)-1		5.0E-04		49	53	102	2.24E+04	2.24E+04
Jug(0)-1	1	5.0E-04	0.5	68	60	128	2.82E+04	2.72E+04
Jug(0)-2		5.0E-04		61	58	119	2.62E+04	
Jug(0)-3		5.0E-04		64	69	133	2.93E+04	
Jug(0)-4		5.0E-04		56	58	114	2.51E+04	
Jug(23)-1	23	5.0E-04	12.5	48	63	111	2.44E+04	2.40E+04
Jug(23)-2		5.0E-04		44	48	92	2.02E+04	
Jug(23)-3		5.0E-04		60	75	135	2.97E+04	
Jug(23)-4		5.0E-04		48	51	99	2.18E+04	
Jug (49)-1	49	5.0E-04	40.4	89	94	183	4.03E+04	3.17E+04
Jug (49)-1		5.0E-04		78	86	164	3.61E+04	
jug (49)-2		5.0E-04		61	68	129	2.84E+04	
Jug (49)-3		5.0E-04		62	73	135	2.97E+04	
Jug (49)-4		5.0E-04		65	74	139	3.06E+04	
jug (57)-1	57	5.0E-04	44.8	58	61	119	2.62E+04	2.16E+04
jug (57)-2		5.0E-04		43	50	93	2.05E+04	
jug (57)-3		5.0E-04		43	40	83	1.83E+04	
jug (57)-4		5.0E-04		47	51	98	2.16E+04	
jug (58)-2	58	1.0E+00	45.3	23	25	48	5.28E+00	1.17E+01
Jug (58)-3		1.0E+00		79	86	165	1.82E+01	
dummy value	0.5		0.3				0.00E+00	0.00E+00
1.5	1.5	1.0E-03	0.8	4	5	9	9.90E+02	9.90E+02
2	2	5.0E-04	1.1	17	18	35	7.70E+03	7.70E+03
3	3	5.0E-04	1.6	43	47	90	1.98E+04	1.98E+04
5	5	5.0E-04	2.7	43	49	92	2.02E+04	2.02E+04
9	9	5.0E-04	4.9	48	36	84	1.85E+04	1.85E+04
11	11	5.0E-04	6.0	34	38	72	1.58E+04	1.58E+04
12.5	12.5	5.0E-04	6.8	37	43	80	1.76E+04	1.76E+04

23	23	5.0E-04	12.5	42	57	99	2.18E+04	2.18E+04
24	24	5.0E-04	13.0	45	45	90	1.98E+04	2.93E+04
24.5	24.5	5.0E-04	13.3	50	55	105	2.31E+04	2.71E+04
25	25	5.0E-04	13.6	41	49	90	1.98E+04	1.98E+04
25.5	25.5	5.0E-04	13.8	33	42	75	1.65E+04	1.65E+04
26	26	5.0E-04	14.1	53	54	107	2.35E+04	2.35E+04
26.5	26.5	5.0E-04	14.4	45	46	91	2.00E+04	2.00E+04
27	27	5.0E-04	14.7	35	43	78	1.72E+04	1.72E+04
27.08	27.08	5.0E-04	15.1	55	59	114	2.51E+04	2.51E+04
27.17	27.17	5.0E-04	15.6	52	84	136	2.99E+04	2.99E+04
27.25	27.25	5.0E-04	16.1	48	64	112	2.46E+04	2.46E+04
27.33	27.33	5.0E-04	16.5	64	66	130	2.86E+04	2.86E+04
27.5	27.5	5.0E-04	17.5	62	84	146	3.21E+04	3.21E+04
27.67-1	27.67	5.0E-04	18.5	45	64	109	2.40E+04	3.18E+04
27.67-2		5.0E-04		65	87	152	3.34E+04	
27.67-3		5.0E-04		83	89	172	3.78E+04	
28	28	5.0E-04	20.4	53	50	103	2.27E+04	2.27E+04
28.5	28.5	5.0E-04	23.2	44	54	98	2.16E+04	2.16E+04
28.73	28.73	5.0E-04	24.5	54	76	130	2.86E+04	2.86E+04
28.83	28.83	5.0E-04	25.1	58	64	122	2.68E+04	2.68E+04
29	29	5.0E-04	26.1	82	92	174	3.83E+04	3.83E+04
29.17	29.17	5.0E-04	27.1	54	61	115	2.53E+04	2.53E+04
29.5-1	29.5	5.0E-04	28.9	66	69	135	2.97E+04	2.72E+04
29.5-2		5.0E-04		49	75	124	2.73E+04	
29.5-3		5.0E-04		56	53	109	2.40E+04	
29.5-4		5.0E-04		60	66	126	2.77E+04	
29.58	29.58	5.0E-04	29.4	62	67	129	2.84E+04	2.84E+04
29.67-1	29.67	5.0E-04	29.9	53	64	117	2.57E+04	2.87E+04
29.67-4		5.0E-04		69	75	144	3.17E+04	
30.5	30.5	5.0E-04	30.4	70	70	140	3.08E+04	3.08E+04
31	31	5.0E-04	30.6	71	78	149	3.28E+04	3.28E+04
33	33	5.0E-04	31.7	45	47	92	2.02E+04	2.02E+04
35	35	5.0E-04	32.8	76	82	158	3.48E+04	3.48E+04

49-1		49	5.0E-04	40.4	48	60	108	2.38E+04	2.83E+04
49-2			5.0E-04		58	65	123	2.71E+04	
49-3			5.0E-04		63	66	129	2.84E+04	
49-4			5.0E-04		69	85	154	3.39E+04	
	51	51	5.0E-04	41.5	82	66	148	3.26E+04	3.26E+04
	52	52	5.0E-04	42.0	57	58	115	2.53E+04	2.53E+04
	52.5	52.5	5.0E-04	42.3	40	47	87	1.91E+04	1.91E+04
	53	53	5.0E-04	42.6	62	75	137	3.01E+04	3.01E+04
	53.5	53.5	5.0E-04	42.9	32	40	72	1.58E+04	1.58E+04
	54	54	5.0E-04	43.1	76	79	155	3.41E+04	3.41E+04
	54.5	54.5	5.0E-04	43.4	59	66	125	2.75E+04	2.75E+04
	55	55	5.0E-04	43.7	31	37	68	1.53E+04	1.53E+04
	55.5	55.5	5.0E-04	43.9	59	56	115	2.53E+04	2.53E+04
56-1		56	5.0E-04	44.2	58	64	122	2.68E+04	2.58E+04
56-3			5.0E-04		69	66	135	2.97E+04	
56-4			5.0E-04		51	44	95	2.09E+04	
	56.5	56.5	5.0E-04	44.5	46	41	87	1.91E+04	1.91E+04
57-1		57	5.0E-04	44.8	61	47	108	2.38E+04	2.16E+04
57-2			5.0E-04		38	44	82	1.80E+04	
57-3			5.0E-04		55	56	111	2.44E+04	
57-4			5.0E-04		43	49	92	2.02E+04	
	58	58	5.0E-04	45.3	49	60	109	2.40E+04	2.40E+04
	59	59	5.0E-03	45.8	53	64	117	2.57E+03	2.57E+03
	61	61	5.0E-03	46.9	24	47	71	1.56E+03	1.56E+03
	71	71	1.0E-02	52.4	40	50	90	9.90E+02	9.90E+02
	74	74	1.0E-02	54.0	38	42	80	8.80E+02	8.80E+02
	76	76	1.0E-02	55.1	30	36	66	7.26E+02	7.26E+02
	76.5	76.5	1.0E-02	55.3	34	40	74	8.14E+02	8.14E+02
	77	77	1.0E-02	55.6	42	44	86	9.46E+02	9.46E+02
	77.5	77.5	1.0E-02	55.9	38	43	81	8.91E+02	8.91E+02
78-1		78	1.0E-02	56.2	37	43	80	8.80E+02	8.17E+02
78-2			1.0E-02		37	42	79	8.69E+02	
78-3			1.0E-02		30	48	78	8.58E+02	

78-4			1.0E-02		28	32	60	6.60E+02	
	78.5	78.5	1.0E-02	56.4	45	60	105	1.16E+03	1.16E+03
79-1		79	1.0E-02	56.7	34	54	88	9.68E+02	7.98E+02
79-2			1.0E-02		35	37	72	7.92E+02	
79-3			1.0E-02		28	29	57	6.27E+02	
79-4			1.0E-02		36	37	73	8.03E+02	
	79.05	79.05	5.0E-03	57.0	24	25	49	1.08E+03	1.08E+03
	79.08	79.08	1.0E-03	57.2	5	6	11	1.21E+03	1.21E+03
	79.12	79.12	5.0E-03	57.4	24	27	51	1.12E+03	1.12E+03
	79.17	79.17	5.0E-03	57.7	22	20	42	9.24E+02	9.24E+02
	79.2	79.2	5.0E-03	57.8	29	19	48	1.06E+03	1.06E+03
	79.25	79.25	1.0E-02	58.1	34	40	74	8.14E+02	8.14E+02
	79.5	79.5	5.0E-02	59.6	35	36	71	1.56E+02	1.56E+02
	79.75	79.75	1.0E-01	61.0	89	93	182	2.00E+02	2.00E+02
	80	80	1.0E-01	62.4	105	123	228	2.51E+02	2.51E+02
	80.25	80.25	1.0E-01	63.8	77	78	155	1.71E+02	1.71E+02
	80.5	80.5	1.0E-01	65.3	75	89	164	1.80E+02	1.80E+02
	80.67	80.67	1.0E-01	66.2	82	91	173	1.90E+02	1.90E+02
	80.82	80.82	1.0E-01	67.1	70	73	143	1.57E+02	1.57E+02
81-1		81	1.0E-01	68.1	72	88	160	1.76E+02	1.61E+02
81-2			1.0E-01		56	66	122	1.34E+02	
81-3			1.0E-01		62	66	128	1.41E+02	
81-4			1.0E-01		86	91	177	1.95E+02	
	82	82	5.0E-02	68.7	46	51	97	2.13E+02	2.13E+02
	84	84	5.0E-02	69.8	175	189	364	8.01E+02	8.01E+02
	95	95	1.0E-01	75.7	207	255	462	5.08E+02	5.08E+02
	97	97	5.0E-02	76.8	161	182	343	7.55E+02	7.55E+02
98-1		98	5.0E-02	77.4	144	171	315	6.93E+02	6.96E+02
98-2			5.0E-02		138	163	301	6.62E+02	
98-3			5.0E-02		116	110	226	4.97E+02	
98-4			5.0E-02		203	220	423	9.31E+02	
	98.05	98.05	5.0E-02	77.6	172	185	357	7.85E+02	7.85E+02
	98.08	98.08	5.0E-02	77.8	170	159	329	7.24E+02	7.24E+02

98.12	98.12	5.0E-02	78.0	181	182	363	7.99E+02	7.99E+02
98.17	98.17	5.0E-02	78.3	161	177	338	7.44E+02	7.44E+02
98.2	98.2	5.0E-02	78.5	135	160	295	6.49E+02	6.49E+02
98.25	98.25	5.0E-02	78.8	91	91	182	4.00E+02	4.00E+02
98.33-1	98.33	1.0E-01	79.2	42	46	88	9.68E+01	1.10E+02
98.33-2		1.0E-01		52	55	107	1.18E+02	
98.33-3		1.0E-01		44	50	94	1.03E+02	
98.33-4		1.0E-01		48	63	111	1.22E+02	
98.5	98.5	1.0E-01	80.2	81	78	159	1.75E+02	1.75E+02